UNIVERSIDADE
BEIRA INTERIOR

Topological Optimization of Tubular Elements Subject to Torsion

"Versão final após a defesa"

Nour Alhag

Dissertação para obtenção do Grau de Mestre em

Engenharia Civil: Estruturas e Construção

(2º ciclo de estudos)

Orientador: Prof. Doutor Luís Filipe Almeida Bernardo

Co-orientador: Doutor. Tiago Pinto Ribeiro

maio de 2025

Declaração de Integridade

Eu, Nour Alhag , que abaixo assino, estudante com o número de inscrição M11409 de 2º ciclo (Mestrado) em Engenharia Civil da Faculdade das Engenharias, declaro ter desenvolvido o presente trabalho e elaborado o presente texto em total consonância com o **Código de Integridades da Universidade da Beira Interior**.

Mais concretamente afirmo não ter incorrido em qualquer das variedades de Fraude Académica, e que aqui declaro conhecer, que em particular atendi à exigida referenciação de frases, extratos, imagens e outras formas de trabalho intelectual, e assumindo assim na íntegra as responsabilidades da autoria.

Universidade da Beira Interior, Covilhã 16 /05 /2025

Acknowledgments

Firstly, I would like to express my profound gratitude to my supervisor, Professor Dr. Luís Filipe Almeida Bernardo, for his unwavering support, invaluable guidance, and dedicated mentorship throughout this work. His contributions have been essential in the completion of this dissertation.

I would also like to express my deepest gratitude to my parents and brothers for their unwavering support throughout my life, without which this achievement would not have been possible.

I would also like to express my deepest gratitude to my husband and children, for their unwavering support and encouragement throughout this endeavor. I would also like to express my profound appreciation to all my professors at UBI.

To all my fellow students, I extend my sincerest thanks for your assistance and companionship.

Resumo

A presente dissertação investiga a otimização topológica de elementos tubulares sujeitos à torção. A investigação concentra-se na aplicação de um software de elementos finitos comercial avançado, normalmente utilizado nas indústrias automóvel e aeroespacial, numa aplicação em estruturas de engenharia civil.

Os objetivos desta investigação são avaliar a viabilidade da utilização de software comercial para o projeto estrutural de estruturas de engenharia civil e validar a utilização da análise de elementos finitos não lineares (NLFEA) após otimização elástica linear. Para tal, foi modelado um tubo comercial de parede fina e selecionado como caso de estudo e o estudo inclui a convergência da malha e a eficiência computacional. A otimização da topologia é realizada para uma fração de volume de (60%). Posteriormente, a geometria otimizada é sujeita a análises não lineares, com o objetivo de avaliar o seu desempenho sob carga de torção. A análise indica que, numa fração de volume de 60%, o tubo otimizado leva a uma redução de 32,5% na resistência ao torque.

Palavras-chave

Método dos Elementos Finitos; Otimização Topológica; Aço; Tubo; Torção; Análise Não Linear.

Abstract

The present dissertation investigates the topological optimization of tubular elements under torsional loading. It focuses on the application of advanced commercial finite element software typically employed in the automotive and aerospace industries, to an application in civil engineering structures.

The objectives of this research are to evaluate the feasibility of using commercial software for the structural design of civil engineering structures and to validate the use of nonlinear finite element analysis (NLFEA) following linear elastic optimization. To that end, a thin-walled commercial pipe is selected as the case study and the study includes mesh convergence and computational efficiency. The topology is optimized for volume fraction (60%). The optimized geometry is then subjected to non-linear analysis to assess its performance under torsion. The analysis indicates that at a volume fraction of 60%, the optimized pipe leads to a 32.5% decrease in torque resistance.

Keywords

Finite Element Method; Topology Optimization, Steel; Non-linear Analysis; Pipe ; Torsion.

Index

List of Figures

List of Tables

List of Acronyms

AM	Additive Manufacturing
FEM	Finite Element Method
NLFEA	Nonlinear Finite Element Analyses
TO	Topology Optimisation
SIMP	Solid isotropic microstructure with penalization

List of Symbols

A_m	Area bounded by the center line of the wall
D	Diameter of the pipe.
E	Modulus of elasticity
fy	Yield strength
fu	Ultimate strength
G	Shear modulus
I_0	Polar moment of inertia.
L	Length of the pipe
R_m	Mean radius of the cross-section.
R_1	Inner radius of the pipe.
$R2$	Outer radius of the pipe.
t	Wall thickness of the thin-walled pipe
τ_{max}	The maximum shear stress
T_R	Torque resistance
s	Perimeter of the centerline of the wall
v	Poisson's ratio in elastic stage
φ	Angle of twist per unit length

1 Introduction

1.1 Motivation

The structural optimization [1], in terms of the sections utilized, has proven to be a particularly arduous task in fixed structures in an ocean environment. These structures are typically composed of thick tubular steel elements that are connected by welding [2]. Given their substantial dimensions, the rigidity of these connections, and the thermal variations of the ocean environment, these elements are subjected to a considerable amount of torsion [3],[4],[5].This behavior renders the optimization of sections considerably more challenging, a task that is more suited to tensioned, compressed, or bent elements.

Notwithstanding the potential benefits of topology optimization [6],[7], including material savings, improved performance, and advances in manufacturing, its adoption in civil engineering, particularly in the context of tubular elements, remains limited. The optimization of tubular elements faces several challenges. These methods often involve complex calculations and advanced software, especially when considering nonlinear behavior. However, experimental data concerning the topology optimization of tubular elements under torsion is highly scarce. Conversely, a considerable number of papers have been published on finite element methods [8],[9].

The following investigation will assess the possibility of employing commercial software, which is commonly used in the automotive and aerospace industries, for the structural design of civil engineering structures. This work will focus on tubular steel members under torsion[10].

1.2 Objective of dissertation

The objective of the current research endeavors is twofold: first, to assess the feasibility of employing commercial software commonly used in the automotive and aerospace industries for the structural design of civil engineering structures and second, to validate the utilization of nonlinear finite element analyses (NLFEA) [11],subsequent to the linear elastic optimization stage . Additionally, the research seeks to provide studies that address mesh convergence and efficiency.

1.3 Followed Procedure

In this investigation, numerical methods are employed[12], namely the use of finite element software incorporating topological optimization algorithms, to optimize the geometry of tubular elements under torsion. For this reason, a thin-walled commercial pipe was selected for the study. Optimizations were executed for volume fraction (60%). In the context of the present study, the SIMP (Solid Isotropic Microstructure with Penalty) method [13], with a penalty factor of 3 was chosen and solved with the Moving Asymptotes method. The objective was to minimize the maximum design response values. The non-optimizable domain was established through the delineation of ring regions at the extremities of

the pipe. Hence, non-linear analyses of the optimized solution were then conducted to ascertain its response [14], [15].

1.3.1 Formalization of the problem

The topology optimization problem under consideration can be outlined as follows:
consider a given design domain Ω, within which the material distribution is expressed by the density variable ρ(x). Hence, a minimization problem is defined for the objective function F, the state field is represented by **u**, and the constraints are denoted by G, with Go ≤ 0 representing the volume constraint and Gi ≤ 0 representing the remaining constraints.

$$\min \{F\} \tag{1}$$

$$F = F(\mathbf{u}(\rho), \rho) = \int_{\Omega} f(\mathbf{u}(\rho), \rho) dV \tag{2}$$

$$G_0(\rho) = \int_{\Omega} \rho(x) dV - V_0 \leq 0 \tag{3}$$

$$G_i(\mathbf{u}(\rho), \rho) \leq 0, i = 1, \ldots, M \tag{4}$$

$$\rho(x) = \{0, 1\}, \forall x \, \Omega \tag{5}$$

1.4 Outline of dissertation

This dissertation is divided into 4 chapters. The present chapter aims to provide an introduction to the research, highlight the objectives and summarize the modelling and analysis process. In the Chapter 2, the definition of geometry of the case study, and the procedure for selecting a thin-walled commercial pipe are elucidated.

The chapter 3 is dedicated to the exposition of the process, encompassing the presentation of the modeling and linear analysis steps, the application of constraints and loads, and the study of mesh convergence.

The objective of Chapter 4 is to provide a comprehensive explanation of the optimization process with volume fraction reduction and the optimization results with linear analysis.

The Chapter 5 will present the optimization results with linear analysis and non-linear analyses of the optimized pipe, along with the conclusions that were derived from these analyses.

2 Case-Study

2.1 Geometrical definition

The initial step in this procedure is the selection of a thin-walled commercial pipe.

The following rule is used to determine whether a section can be treated as thin-walled:

$$\frac{R_m}{t} > 20 \qquad (1)$$

Where:

- R_m: Mean radius of the cross-section. It represents the distance from the center of the section to the midline of the wall.
- t: Thickness of the wall.

$$R_m = (406.4/2)-4=199.2 \text{ mm}$$

$$t<9.96mm$$

$$t=8\ mm$$

The pipe in question was obtained from the "CHAGAS" table, see Table 1, with a diameter of 406.4 mm.

Table 1. "CHAGAS" table (hot-rolled structural round pipes).

CHAGAS

Tubo Estrutural Laminado a Quente
Redondo

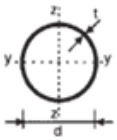

Norma Dimensional - EN 10210-1
Material S355 J2 H

d mm	t mm	M Kg/m	A cm²	L cm²	i cm	Wel cm³	Wpl I en cm³	It cm³	Ct cm³	S m²/t
193,7	6,3	29,1	37,09	1630	6,629	168,3	221,3	3260	336,6	20,9
193,7	8,0	36,6	46,67	2016	6,572	208,1	276	4031	416,2	16,61
193,7	10,0	45,3	57,71	2442	6,504	252,1	337,8	4883	504,2	13,43
193,7	12,0	53,8	68,5	2839	6,438	293,2	396,8	5678	586,3	11,32
193,7	14,0	62	79,04	3210	6,373	331,4	453	6419	662,8	9,808
219,1	3,6	19,1	24,37	1415	7,62	129,2	167,2	2830	258,4	35,98
219,1	5,0	26,4	33,63	1928	7,572	176	229,2	3856	352	26,07
219,1	6,3	33,1	42,12	2386	7,527	217,8	285,4	4772	435,6	20,82
219,1	8,0	41,6	53,06	2960	7,469	270,2	356,7	5919	540,3	16,53
219,1	10,0	51,6	65,69	3598	7,401	328,5	437,6	7197	656,9	13,35
219,1	12,0	61,3	78,07	4200	7,334	383,4	515,3	8400	766,8	11,23
244,5	5,0	29,5	37,62	2699	8,469	220,7	286,8	5397	441,5	26,01
244,5	6,0	35,3	44,96	3199	8,435	261,6	341,4	6397	523,3	21,77
244,5	8,0	46,7	59,44	4160	8,366	340,3	447,6	8321	680,1	16,46
244,5	10,0	57,8	73,67	5073	8,298	415	550,2	10150	830	13,28
244,5	12,0	68,8	87,65	5938	8,231	485,8	649,3	11880	971,5	11,16
244,5	14,0	79,6	101,4	6758	8,164	552,8	744,7	13520	1106	9,652
273,0	5,0	33	42,1	3781	9,477	277	359,2	7562	554	25,95
273,0	6,0	39,5	50,33	4487	9,442	328,7	427,8	8974	657,4	21,71
273,0	8,0	52,3	66,6	5852	9,373	428,7	562	11700	857,4	16,4
273,0	10,0	64,9	82,62	7154	9,305	524,1	692	14310	1045	13,22
273,0	12,0	77,2	98,39	8396	9,237	615,1	818	16790	1230	11,1
273,0	14,0	89,4	113,9	9580	9,17	701,8	940	19160	1404	9,591
323,9	5,0	39,3	50,09	6369	11,28	393,3	508,5	12740	786,6	25,88
323,9	6,0	47	59,92	7572	11,24	467,6	606,4	15140	935,2	21,63
323,9	8,0	62,3	79,39	9910	11,17	611,9	798,5	19820	1224	16,33
323,9	10,0	77,4	98,61	12160	11,1	750,7	985,7	24320	15,01	13,14
323,9	12,0	92,3	117,6	14320	11,04	884,2	1168	28640	1768	11,02
323,9	14,0	107	136,3	16400	10,97	1012	1345	32790	2025	9,51
355,6	6,0	51,7	65,9	10070	12,36	566,4	733,4	20140	1133	21,6
355,6	8,0	68,6	87,36	13200	12,29	742,5	966,8	26400	1485	16,29
355,6	10,0	85,2	108,6	16220	12,22	912,5	1195	32450	1825	13,11
355,6	12,0	102	129,5	19140	12,16	1076	1417	38280	2153	10,99
355,6	14,0	118	150,2	21950	12,09	1235	1635	43900	2469	9,472
355,6	16,0	134	170,7	24660	12,02	1387	1847	49330	2774	8,337
406,4	6,0	59,2	75,47	15130	14,16	744,5	962	30260	1489	21,55
406,4	8,0	78,6	100,1	19870	14,09	978	1270	39750	1956	16,24
406,4	10,0	97,8	124,5	24480	14,02	1205	1572	48950	2409	13,06
406,4	12,0	117	148,7	28940	13,95	1424	1867	57870	2848	10,94
406,4	14,0	135	172,6	33260	13,88	1637	2157	66520	3274	9,424
406,4	16,0	154	196,2	37450	13,81	1843	2440	74900	3686	8,288

A pipe with a diameter of 406.4 mm and a length of 5 m was assumed. The geometric characteristics of the pipe are shown in Table 2.

Table 2. The geometrical characteristics of the pipe.

t	8	mm
D	406.4	mm
R_m	199.2	mm
R_1	195.2	mm
R_2	203.2	mm
L	5	m
I_0	397477855.70	mm^4
A_m	124660.4	mm^2

Where

t: Wall thickness of the thin-walled pipe.

D: Diameter of the pipe.

R_m: Mean radius of the cross-section.

R_1: Inner radius of the pipe.

*R*2: Outer radius of the pipe.

L: Length of the pipe.

I_0: Polar moment of inertia.

A_m: Area bounded by the center line of the wall.

2.2 Material definition:

This case study's pipe was made of Grade 50 steel according to the ASTM A572/A572 M standard. This law specifies a minimum yield strength of 345 MPa, the minimal ultimate strength of 450 MPa [10] , see Figure 1.

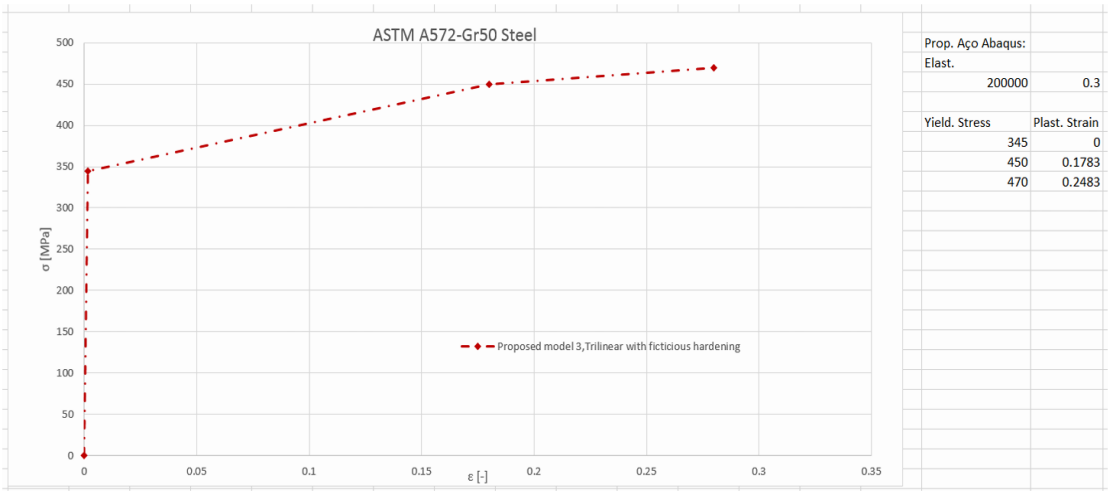

Figure 1.A572 Gr50-Steel law

2.3 Torque Resistance

The second step in the process is to calculate the torque resistance T_R[16]. This is achieved by employing Bredt's first formula for thin-walled closed sections. The formula requires the specification of A_m, which is the area bounded by the centre line of the wall, and t which is the wall thickness.

$$T_R = \tau_{max} * 2 * A_m * t \qquad (2)$$

The maximum shear stress is as follows:

$$\tau_{max} = \frac{fy}{\sqrt{3}} \cong 200 \text{ MPa} \qquad (3)$$

$$T_R = 398.9 \text{ KN. m}$$

3 Modeling

The objective of this section is to provide a comprehensive presentation on the modeling, optimization, and analysis steps involved [10]. To that end, a case study has been selected for examination. The A572 Grade 50 steel pipe with symmetrical holes meticulously drilled along the length of the pipe, thereby creating areas of variation in internal stress, as illustrated in Figure 2, has been selected for analysis. The pipe's dimensions are as follows: a length of 5,000 mm, a diameter of 406.4 mm, and a thickness of 8 mm. It contains 28 holes, each with a diameter of 40 mm. Thay are distributed in seven planes perpendicular to the longitudinal axis, with four holes symmetrically distributed in each plane. It has been determined that the distance between the levels is 500 mm, and the distance from the end of the pipe is 1,000 mm.

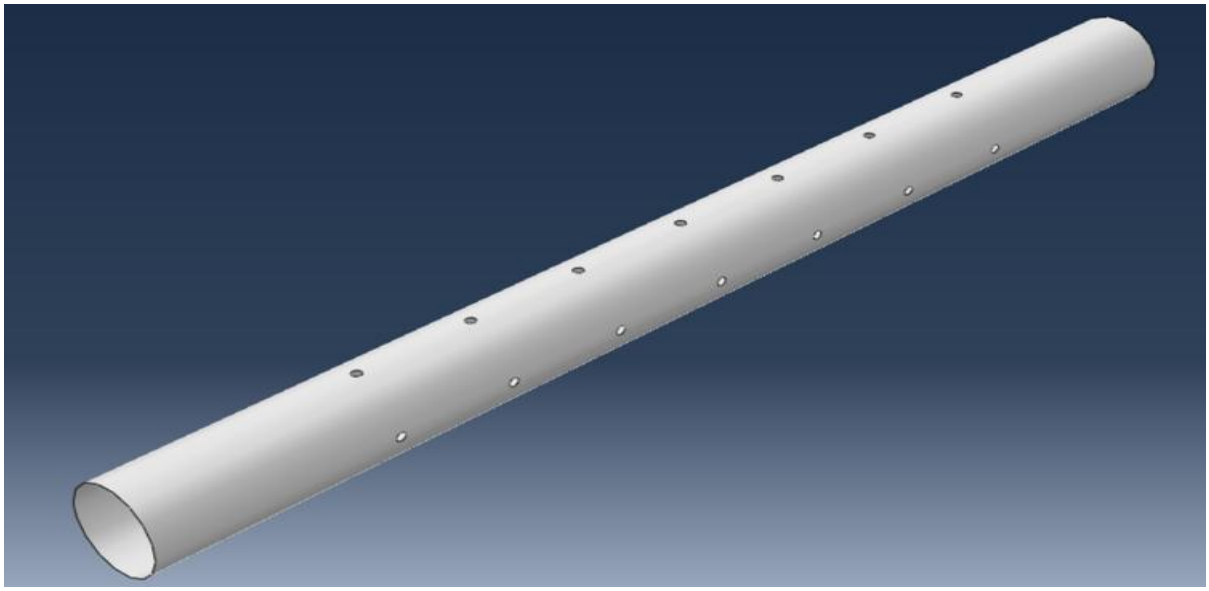

Figure 2. Case-study pipe

3.1 Modelling and (Material) linear Analysis

Because the goal of this analysis is to apply topological optimization, linear analysis was chosen to be used to simplify the process of initial analysis[17],[18]. Subsequent to obtaining the optimized model, nonlinear analysis is utilized to examine the static response of the model. It is important to note that, as by-standard, N, mm and MPa (N/mm^2) units have been used. The chosen software for this work was Abaqus and Tosca for Topology Optimization of Steel [10].

Initially, the file is opened and saved. Subsequently, the path for storing the model files is selected from the "Set Work Directory" option. Thereafter, in the dialog titled "Create Part" the name "work_piece" was defined. In the following steps, "3D" was selected for the modeling space, "Deformable" for the type,

“Shell” for Shape in Base Feature and “extrusion” for Type. The auxiliary grid approximate size has been defined as 1000 mm.

Using “Create Circle: Centre and Perimeter”, the coordinates of the center point (0,0) and one point on the perimeter (0,203.2) are introduced to draw the circle. Within “Edit Base Extrusion” dialog 5000 has been defined for depth. With “Create Datum Plane” one can introduce auxiliary datum plane YZ Plane and XZ Plane. Thereafter, use each plane to draw the circles to create the holes as reported in Figure 3. “Create Cut Extrude” command has been used.

Using “Create Circle: Centre and Perimeter” in the Sketch module. For the hole in the middle of plane the coordinates of the center point (0,0) and one point on the perimeter (0,20) are introduced to draw the circle. The "Linear Pattern" command has been used for the remaining holes. The spacing between the circles and the number of circles is introduced to draw the circles. Accordingly, the task of creating the holes has been accomplished, see Figure 4.

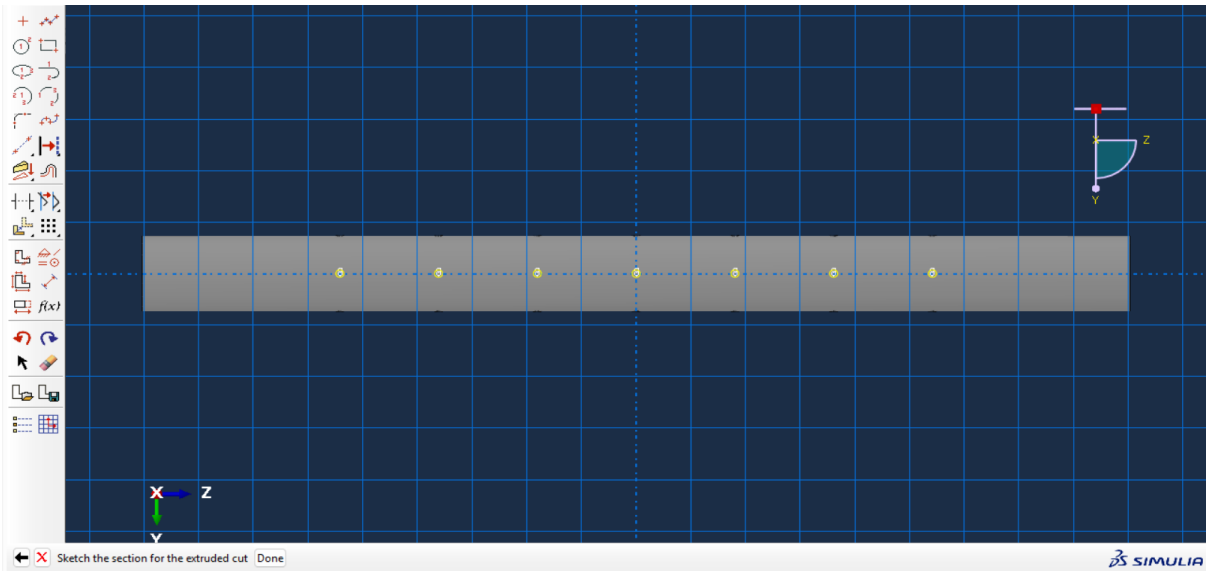

Figure 3. YZ plane

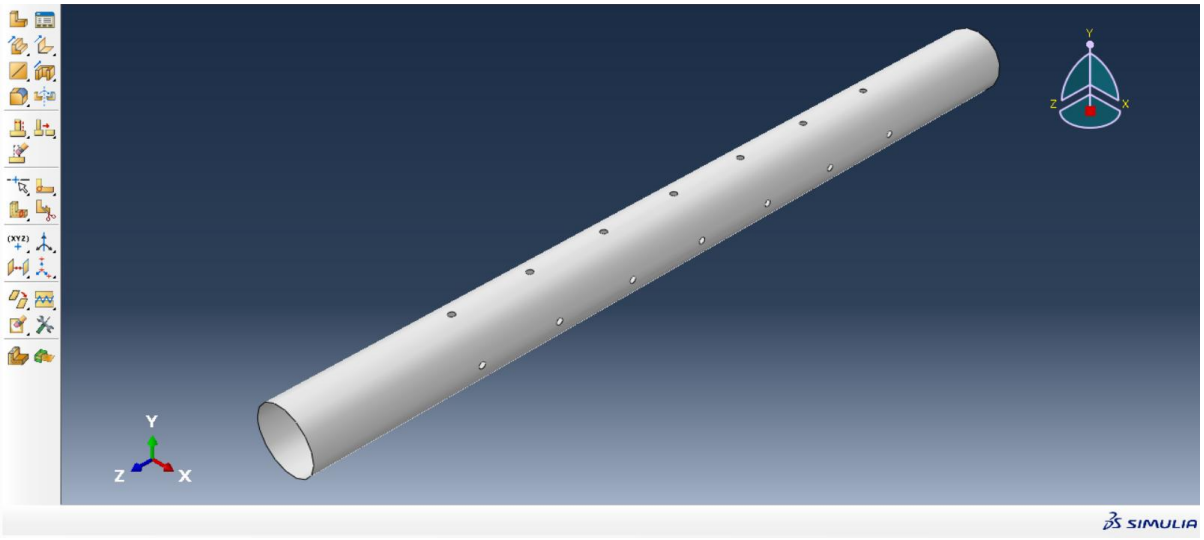

Figure 4. Final defined pipe

It is imperative to consider the pipe ends as non-optimizable domains of the steel pipe , this is essential to ensure the uniform distribution of stress. Hence, the area within a distance of 406.4 mm from the pipe's extremity was be considered non-optimizable domains of the steel pipe. Topological optimization was be implemented within the middle domain.

With “Create Datum Plane” one can introduce an auxiliary datum plane XY Plane with offset 406.4 from the principal plane for the first partition and an auxiliary datum plane XY Plane with offset 4593.6 for the second partition. The “Partition Face: Use Datum Plane” command has been used to create partitions. Partitions for the pipe's edges have been created. These rings are considered non-optimizable domains of the steel pipe. See Figure 5.

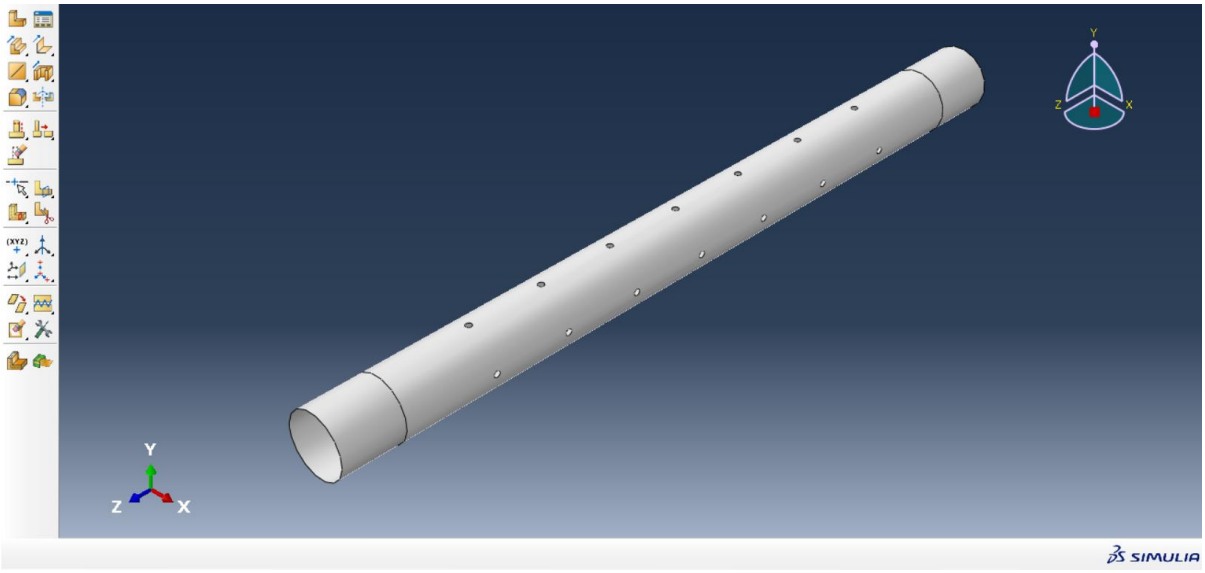

Figure 5.Creating the limits for non-optimizable domains

The linear material law must be inserted within the "Create Material" option of the "Module Property" tool. In the dialog titled "Edit Material" the name " A572 Gr50-Steel " has been defined [10]. The A572 Gr50-Steel constitutive law was initiated by first selecting the Mechanical Elasticity option. Then, the relevant parameters were entered. The values of 200 x 10^3 for Young's modulus and 0.3 for Poisson's ratio have been entered into the appropriate fields.

In the “Create Section” dialog, a section named “pipe” was created, and its Category (Shell) and type (Homogeneous) were defined. After that, the shell thickness was defined as 8 and “A572-Gr50-Steel” was selected as the material. Hence, the "Assign Section" option should be applied after the whole model has been selected and "Done" has been selected. This process is illustrated in Figure 6.

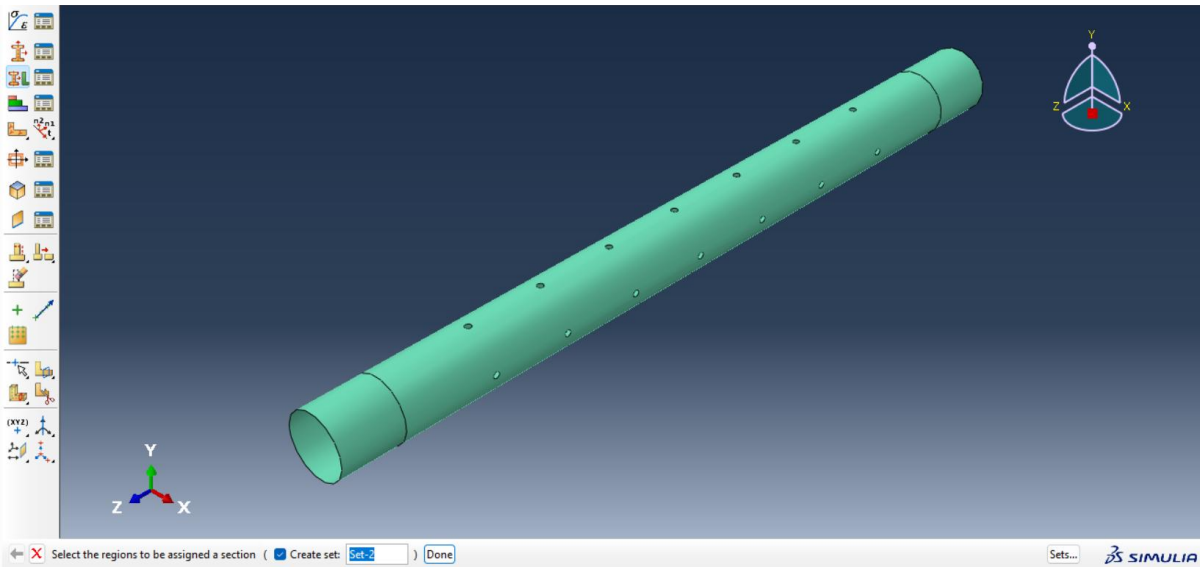

Figure 6.Assigned section to the pipe.

The following step was to "Create Instance" within the Assembly Module. As shown in Figure 7.

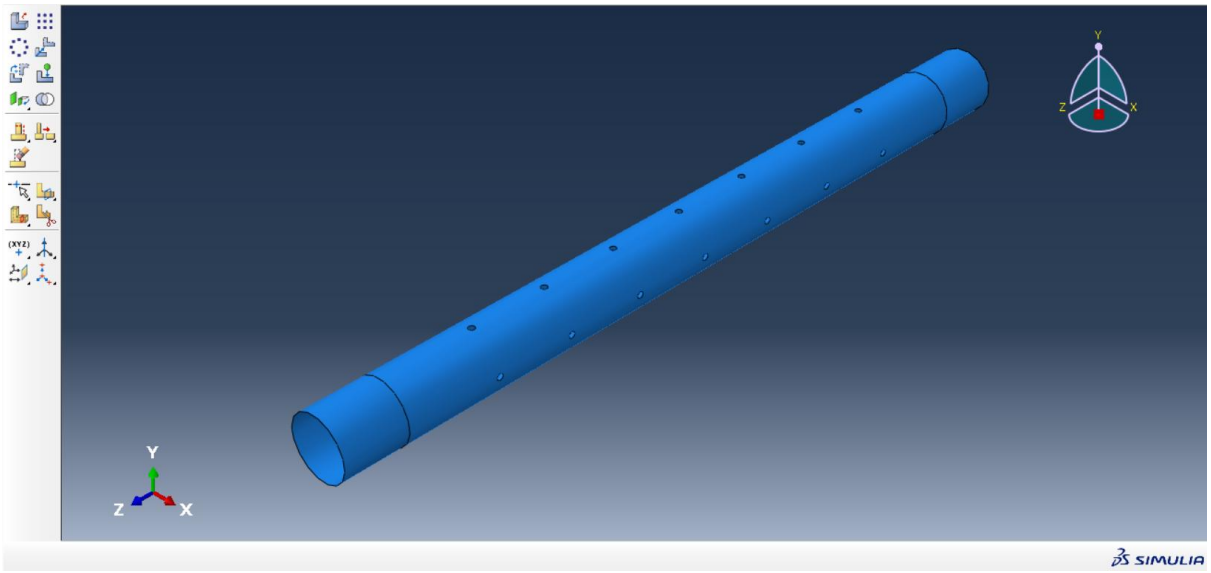

Figure 7.Creating the instance

The "Create Step" option has been selected to define the procedure type as "General," and subsequently as "Static, General". The Maximum number of increments has been defined as 10,000, and the Increment size Initial and Maximum has been set to 0.01.

3.2 Application of constraints and loads

The utilization of a coupling serves to apply loads and boundary conditions to a designated point, which is subsequently propagated to a broader area. In the context of our study, the coupling is employed to apply a force to a reference point (RP) that is coupled to the surface of the pipe's edge.

The reference points RP-1 (0, 0, -406.4) and RP-2 (0, 0, 5406.4) have been created in the Assembly Module. Module Interaction has been activated. In "Create Constraint" dialog Constraint-1 has been defined as the name and Coupling has been selected as the type before continuing to select RP-1 and the opposing surface of the pipe section. The coupling type was set to "kinematic," and all constrained degrees of freedom were activated. The process should be repeated for RP-2, with one modification: only U1 and U2 displacements were constrained in "constrained degrees of freedom". This process is illustrated in Figure 8.

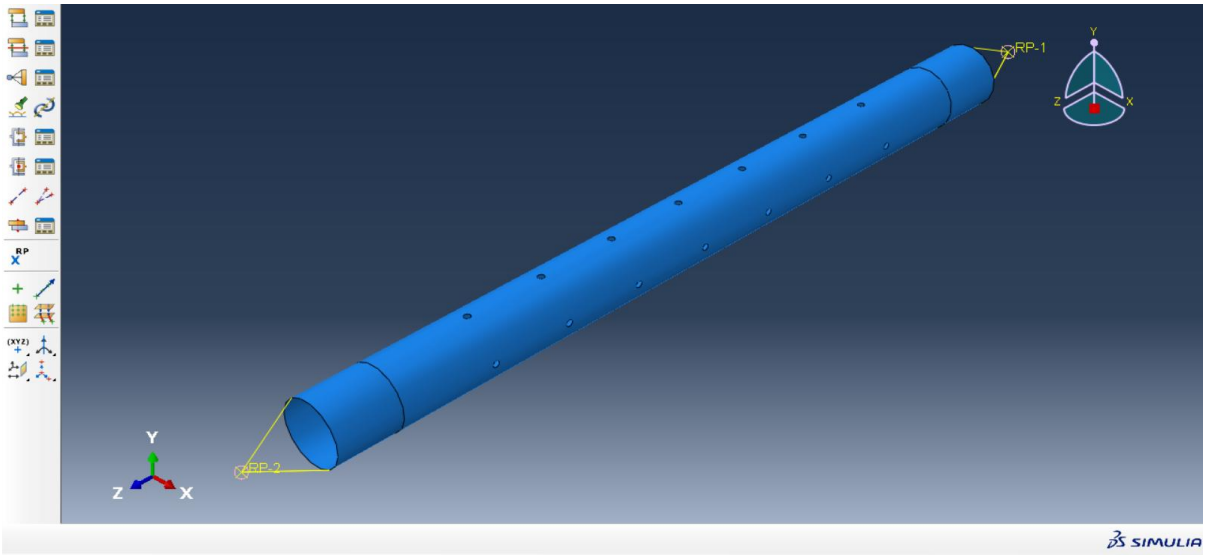

Figure 8.Creating Coupling

The "Create Load" option in the Load Module was selected. The "Moment" has been defined as the name, and the "Moment" has been selected as the types of selected steps, where "Step-1" has been chosen. The category has been set as "Mechanical", After that, PR2 was selected, and a value of 3.98913E+08 was declared for "MC3", see Figure 9.

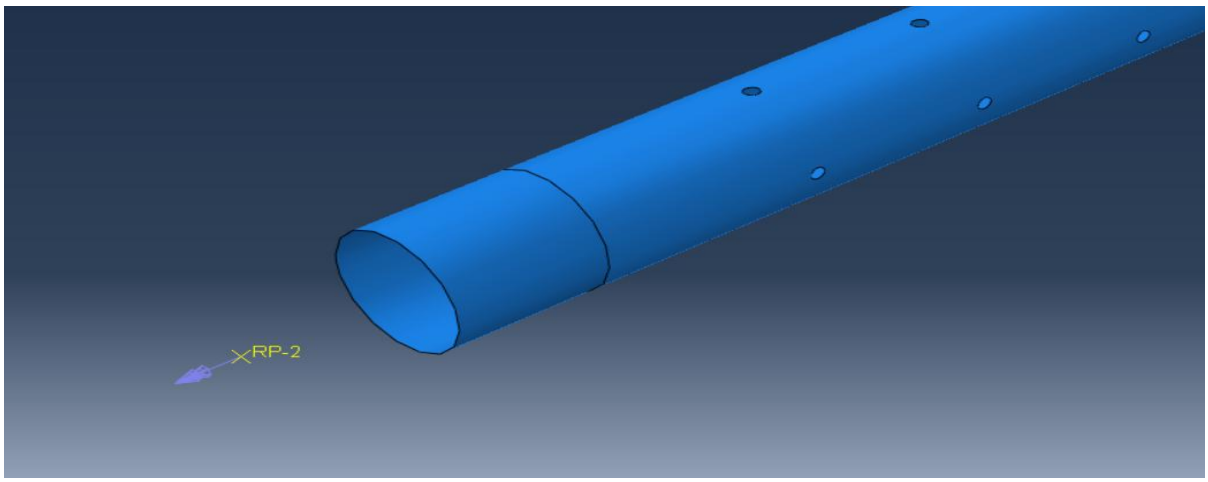

Figure 9.Creating the load

In the Load Module, the “Create Boundary Condition” is activated. Then, “Restrain” was created with the following properties: “Initial” step, “Mechanical” category and “Symmetry / Antisymmetry / Encastre” was the option for “Types for Selected Step”. Following the selection of PR1 the option “Encasrte U1=U2=U3=U4=U5=U6=0“is chosen, See Figure 10.

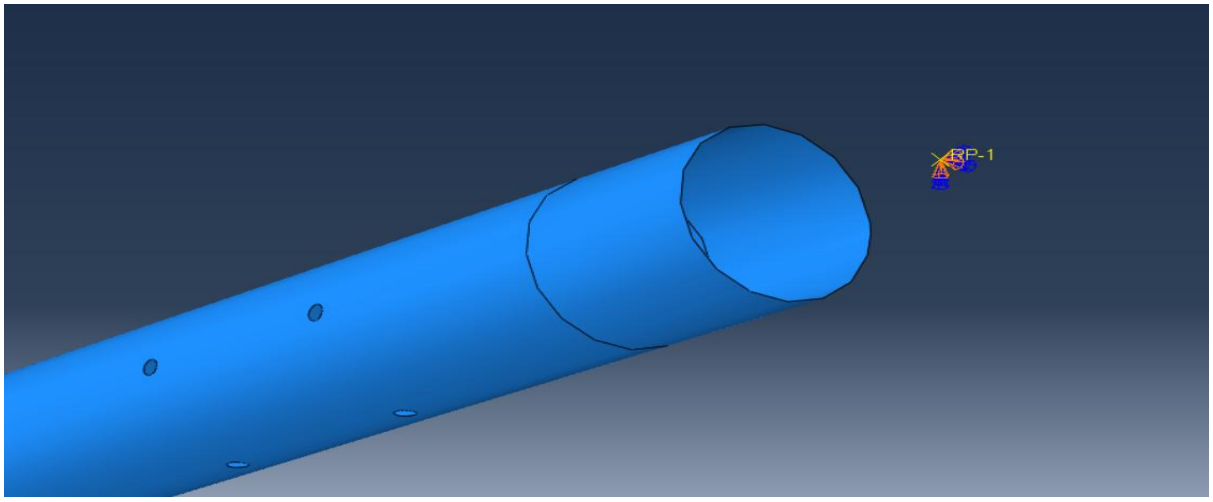

Figure 10.Defined restraints

3.3 Mesh convergence study

The goal of this study is to determine a mesh size that will produce real-world results with a minimum of computational effort. In this study, triangular finite elements were first considered and nine mesh options were tested for the entire pipe to evaluate the most efficient mesh refinement.

Table 3. Tested meshes

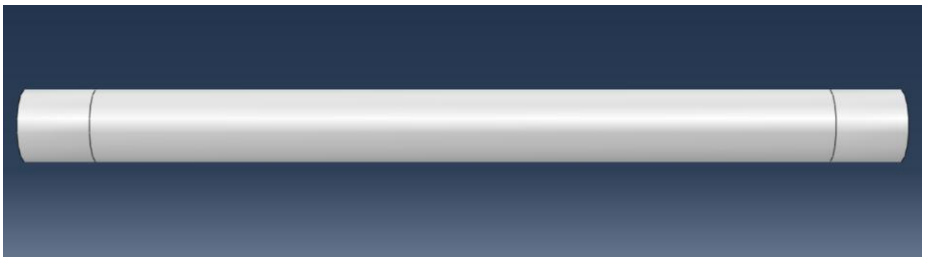	Number of elements
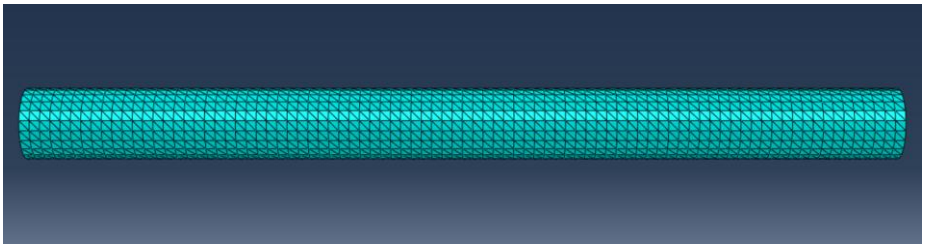	1914 Elements Size 57
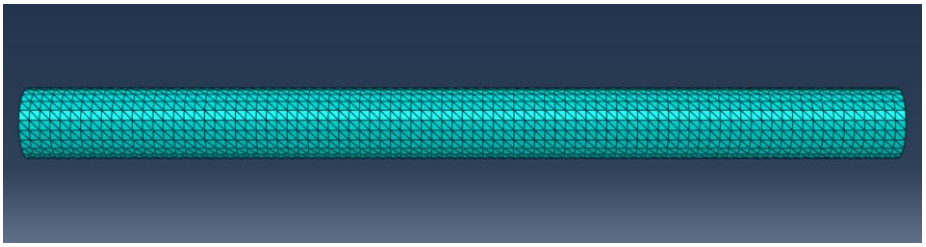	2652 Elements Size 50

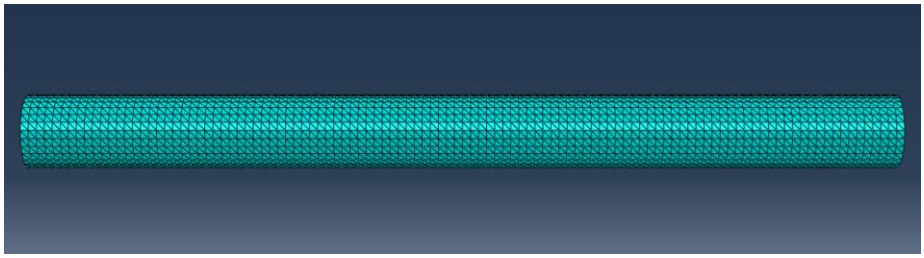

3108 Elements
Size 45

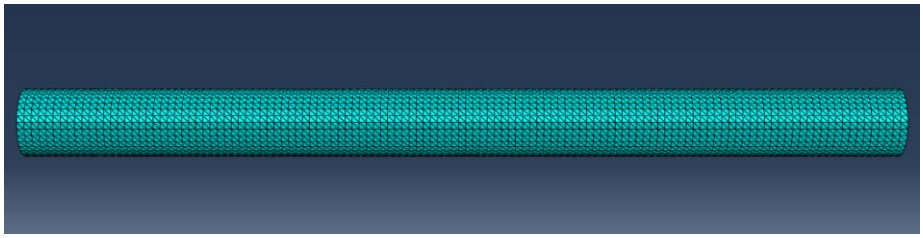

4032 Elements
Size 40

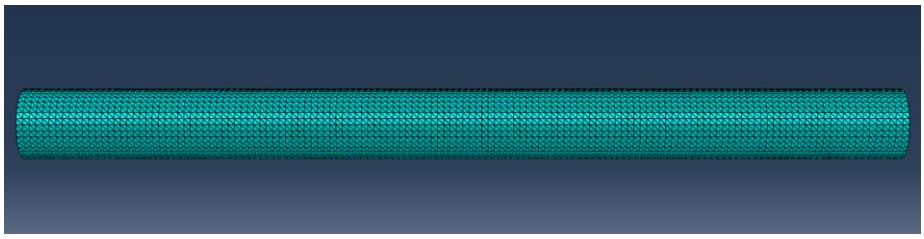

5076 Elements
Size 35

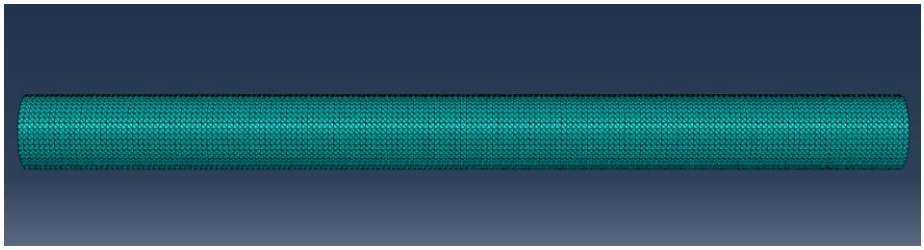

7310 Elements
Size 30

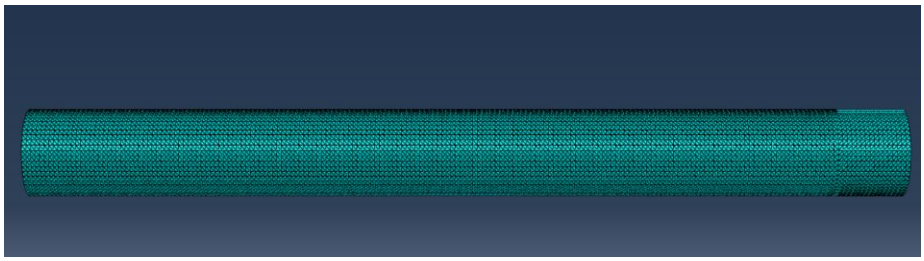

10200 Elements
Size 25

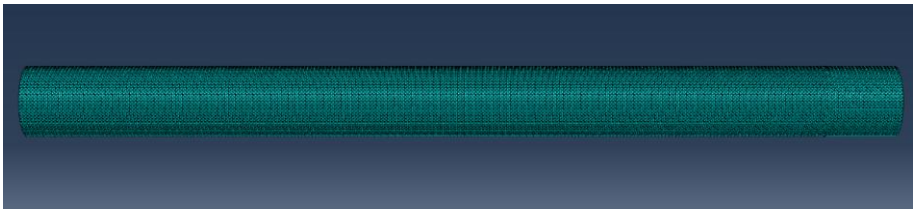

16064 Elements
Size 20

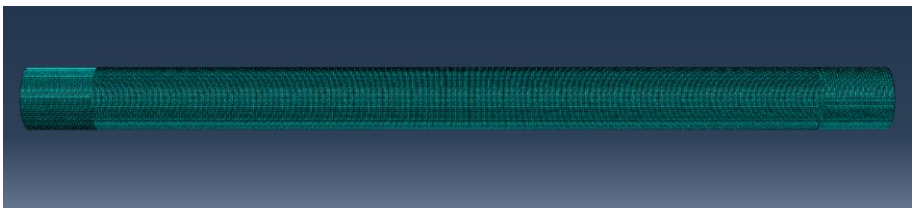

28390 Elements
Size 15

The simulation was repeated, and Von Mises stress values were recorded at the midpoint of the pipe for each mesh level. The following curve has been delineated, see Figure 11.

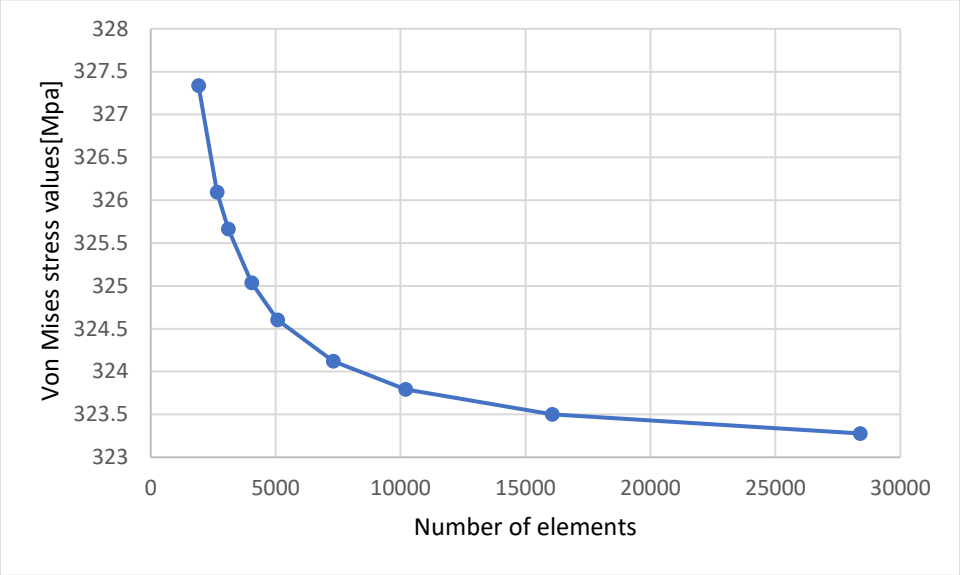

Figure 11. Curve (Von Mises stress values [Mpa], Number of elements)

A value of 20 has been selected for the element size with 16064 elements in the mesh, with the objective of minimizing computational effort[21] . This determination was made through a detailed analysis of the previous curve, which revealed that the mesh level corresponding to the value 20 for element's size produced only a marginal increase in the value of von mises stress. In contrast, a substantial rise in the number of elements was observed.

Ensuring the accuracy and independence of the simulation results from the mesh size is imperative. To this end, it must be noted that the value of φ at the free end of the pipe is the parameter that will be used to compare with results extracted from Abaqus for each level of mesh at a later stage. The value of φ has been calculated using the following formula:

$$\varphi = \frac{Tr*s}{4*A_m^2*G*t} \qquad (4)$$

where:

Tr: torque resistance.
A_m: area bounded by the center line of the wall.
t: Wall thickness of the thin-walled pipe.

φ :angle of twist per unit length.

s perimeter of the centerline of the wall

G shear modulus

$$G = \frac{E}{2(1+\nu)} \qquad (5)$$

$$G \approx 81000\ N/mm^2$$

Modulus of elasticity

$$\mathrm{E} = 210\ 000\ \mathrm{N/mm^2}$$

Poisson's ratio in elastic stage

$$\nu = 0.3$$

For the specified object, the curve (Tr, φ) has been delineated, see Figure 12 . Subsequent analysis was conducted to ascertain the extent of conformity between the theoretical curve provided by Bredt's theory and the curves extracted from Abaqus for the 20 mm and 57 mm mesh levels.

Recording the results extracted from Abaqus allows for the tracking of how the value parameter changes as the mesh is refined [22]. This ensures that the simulation results are accurate and independent of the mesh size.

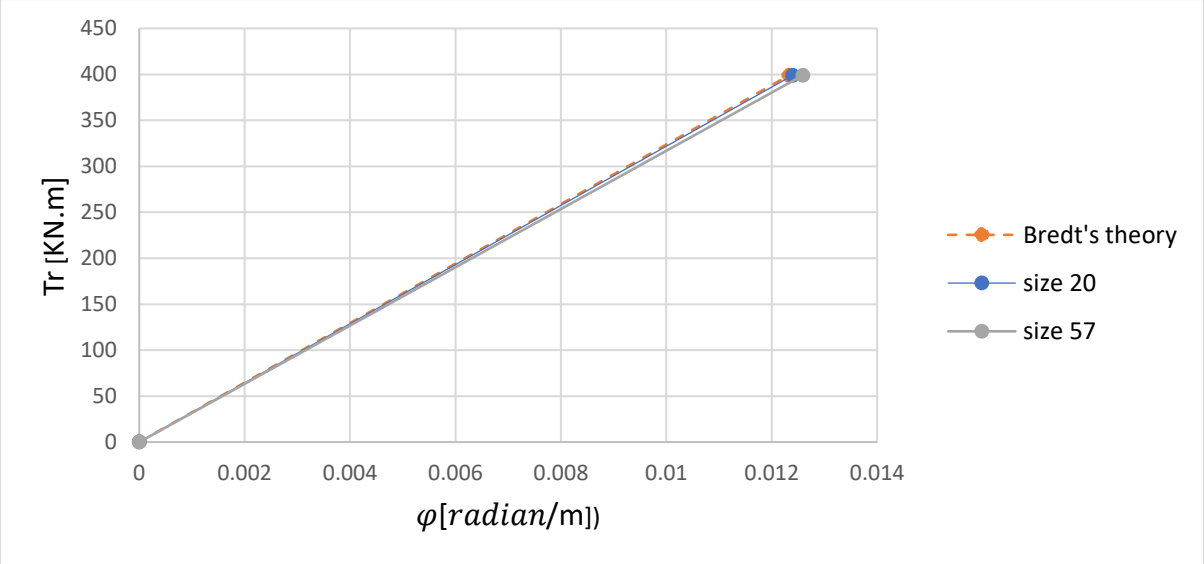

Figure 12. Curve (Tr [KN.m], $\varphi[radian/\mathrm{m}]$)

By studying the curves in Figure 12, it was found that the theoretical straight line matches the same one extracted from Abaqus for the 20 mm mesh level, which means that the simulation results are accurate and independent of the mesh size.

In order to adequately ascertain the level of refinement, it is imperative to take into consideration a range of factors, including but not limited to computational resources and time constraints[20].

In the Mesh Module, the option “Part” was activated and “Seed Part” was selected. The approximate global size has been defined as 20 mm. Following the activation of the "Assign Element Type", the entirety of the model was selected and the option "tri" was chosen. Upon opening the Element Type dialogue, the options "linear" for Geometric Order, "Shell" for Family, and "Tri" Triangular for element shape were selected.

In the Module Job the “Create Job” option was selected. In “Parallelization” page, the option “Use multiple processors” was activated and “4” processors were required to reduce the calculation effort. In the "Job Manager," the "Data Check" option was selected in order to initiate the analysis of the Input File, and the "Monitor" option was subsequently selected in order to access the results. A thorough examination of the obtained results reveals the presence of high local stress points in some finite elements due to numerical error, see Figure 13.

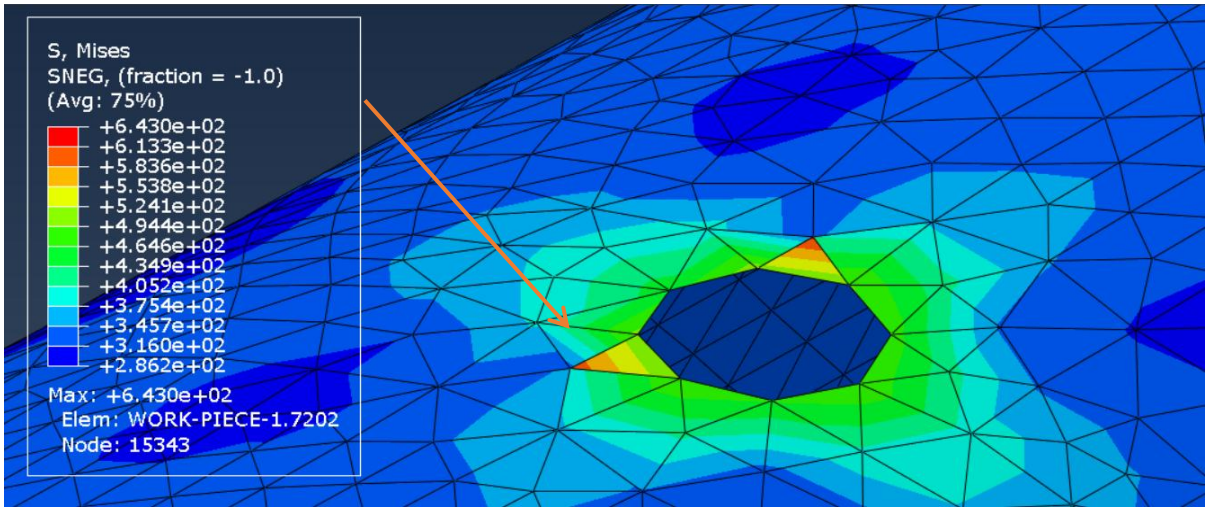

Figure 13 . Result of linear analysis

Following a series of experiments aimed at resolving the issue, the following modifications were implemented.

Partitions for the outer limit of the holes have been created with radius r1 = 80 mm. For this, “Partition Face: Sketch” command has been used and new circle has been drawn with radius of r1= 80 mm in the middle of Sketch module, using “Create Circle: Centre and Perimeter”. The remaining circles have been drawn by using “Linear Pattern" command, Figure 14.

The spacing between the circles and the number of circles is introduced to draw the circles. the geometry is defined as illustrated in Figure 15.

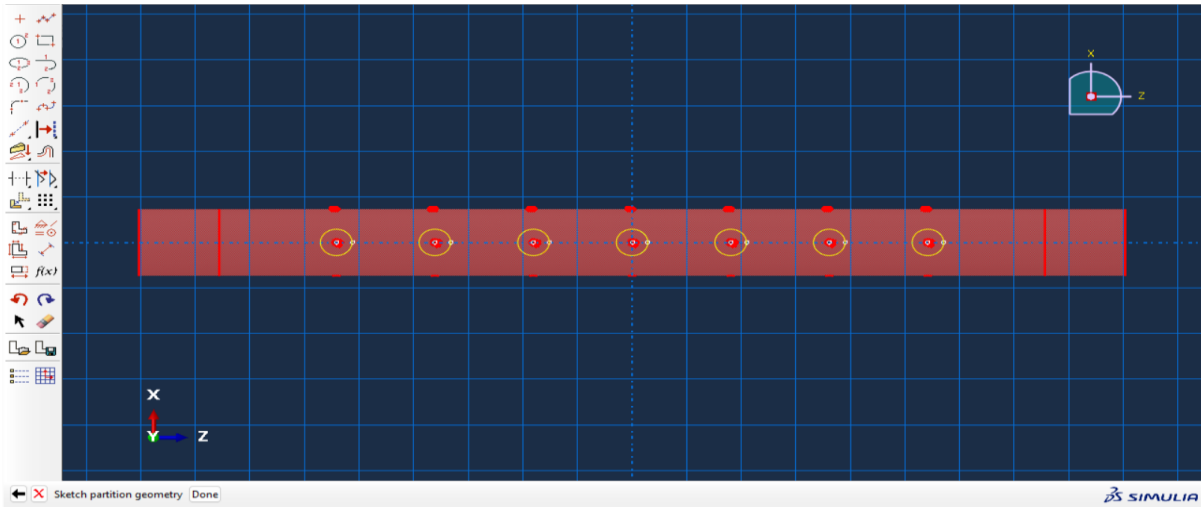

Figure 14 .Creating the partitions

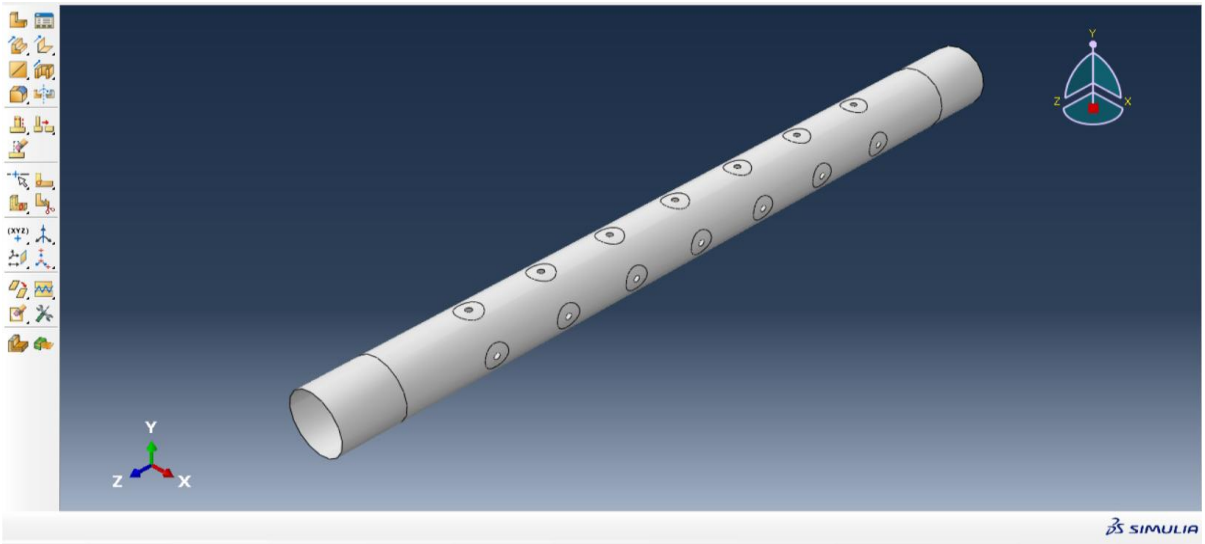

Figure 15 . Partitioned pipe

In the Mesh Module, the option “Part" was activated, and "Seed Part" was selected. The approximate global size has been defined as 5. In the "Assign mesh control" option, the "quad-dominated” was activated after the entire model has been selected. Subsequently, the "Assign Element Type" option was activated, and the entirety of the model was selected. the options "linear" for geometric order, "shell" for family, and "quad" for element shape were selected. Then, the option "Mesh Part" was activated, the selection of the "Yes" option was made to mesh the part, as illustrated in Figure 16.

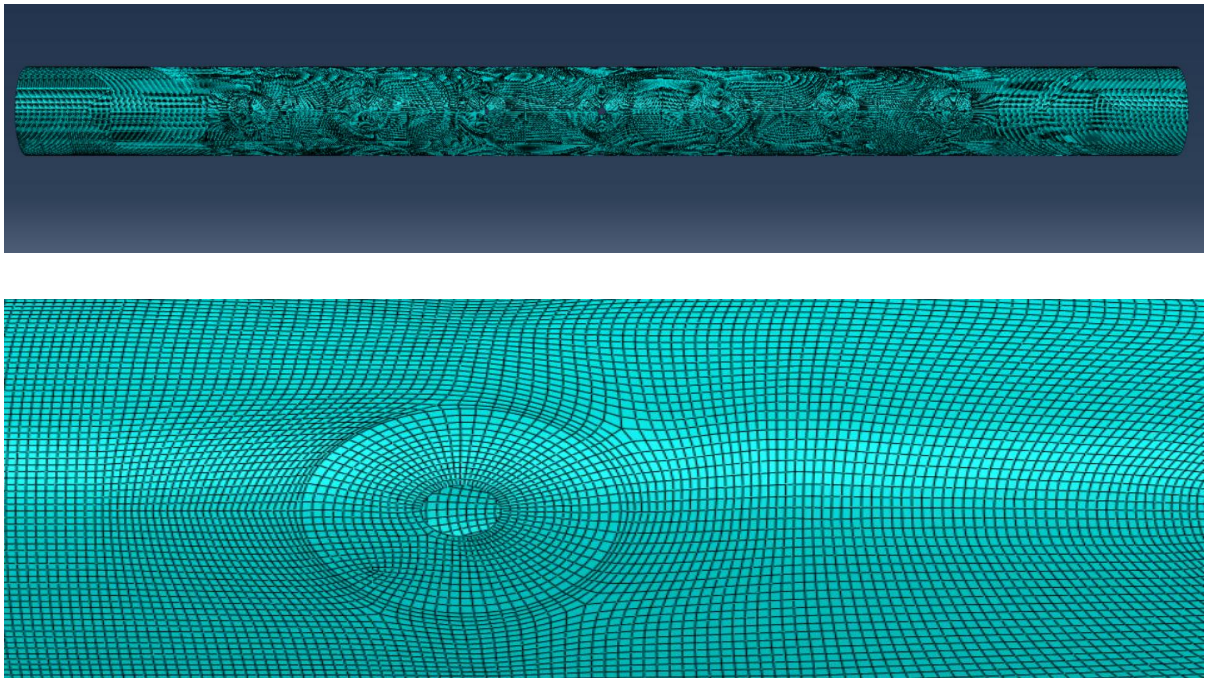

Figure 16 .Meshed pipe

The entire pipe (with 5 mm mesh level) was subjected to topography optimization.

4 Topology Optimisation

The method for TO is designed in the same Abaqus environment and is based on the already modeled geometry. It should be remembered that the basic units used are N, mm and MPa (N/ mm^2).

In the Optimization module, the "Create Optimization Task" option was selected and the task was named "TO". The entire pipe has been selected. After opening the Edit Optimization Task dialog box. The "Advanced" folder is selected. In the "Material Interpolation Technique", the "SIMP" option has been activated [23],[24][25] ,and the Penalty Factor was set to "3", Figure 17.

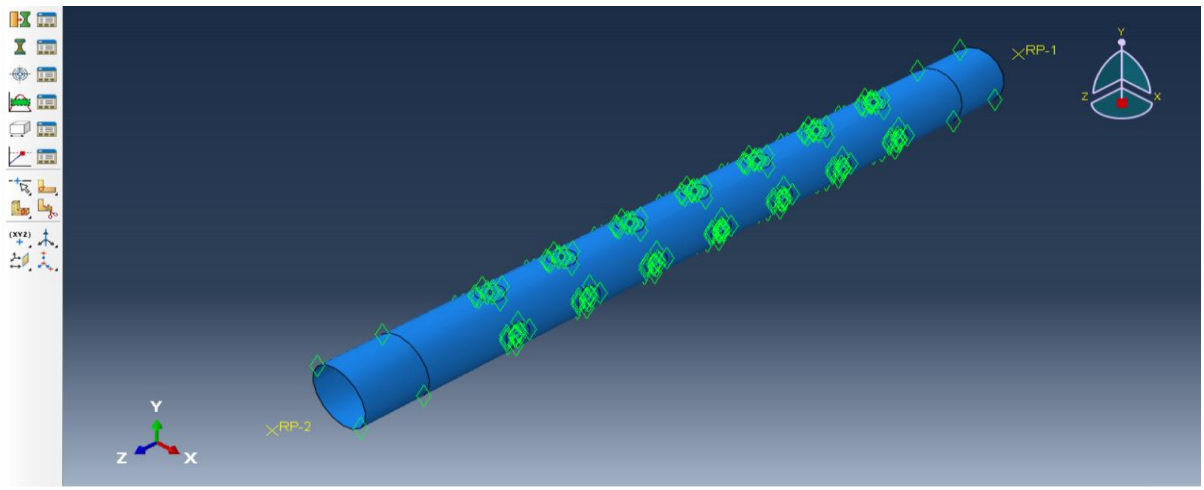

Figure 17 . Creating optimization task

In the optimization module, the "Create Design Response" option was selected and designated "stress." The "Single-term" option was selected for the "Type" field. In the subsequent step, the entire model was selected. The "stress" option was selected in the "Edit Design Response" dialogue box.

Within the optimization module, the "Create Design Response" option was selected, and the name "Volume" was designated. The "Single-term" option was selected for the Type. Upon selecting the "Whole Model" option, the "Volume" option was selected in the "Edit Design Response" dialog box.

In the optimization module, the "Create Objective Function" option was enabled to generate an objective function designated as "Min_Max_Stress"[10].Within the "Edit Objective Function" dialog box, the objective "Minimize the maximum design response values" was selected as the target. To this end, the "Name" field was designated as "stress". An objective function that seeks to minimize the maximum design response is an important optimization formulation. In each design cycle, the Optimization module first identifies the set of weighted design responses that attain the maximum

value, and subsequently endeavors to minimize that design response. In numerous instances, minimizing the maximum design response yields a satisfactory solution because it reduces the maximum of a number of design responses. In the present study, design responses are defined from the stress in multiple regions of the model. The objective is to minimize the maximum design response attempts to minimize the stress in the region that exhibits maximum stress.

In the next step, the optimization module is utilized to generate a constraint, designated as "Red_Vol." Within the "Edit Optimization Constraint" dialog box, under the "Design Response" section, the "Volume" has been selected for the "Name". Additionally, within the "Constrain Response" section, the "Fraction of Initial Value" parameter has been set to "0.6".

The "Create Geometric Restriction" option was enabled within the optimization module. The designated name for this option is "Rings," and the "Frozen area" parameter was selected for the “Type”. Therefore, the non-optimizable domain has been created by defining ring regions at the extremities of the pipe manually, as illustrated in Figure18, 19.

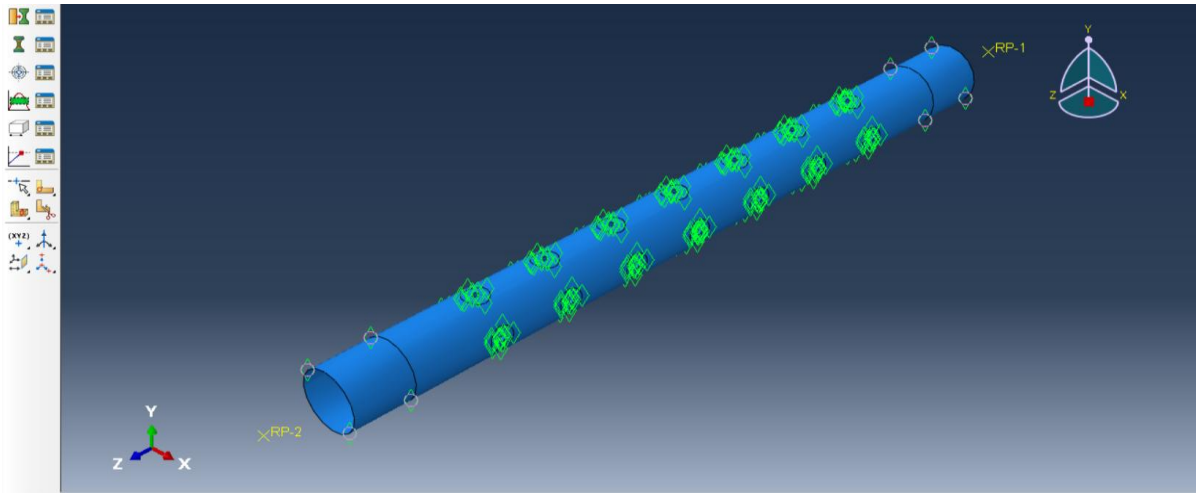

Figure 18. Ring regions as non-optimizable domain

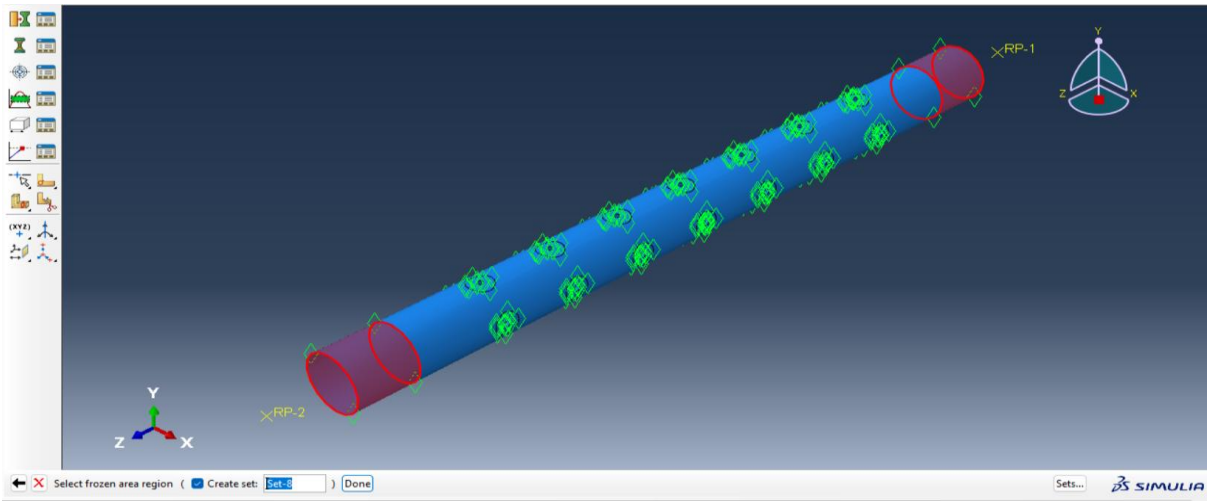

Figure 19. Defined non-optimizable domain

In the Job module, the "Create Optimization Process" option was selected. However, in order to define the optimization process, it was necessary to utilize the "Edit Optimization Process" dialog box. Within the "optimization" folder, the value of "50" was designated for the Maximum cycles, and in the "Parallelization" folder, the "Use multiple processors" option was selected and set to "4". In addition, in the Job module, the Optimization Process Manager module, the "Validate" command has been selected to start the Analysis Input File. After solving all the problems with errors and warnings. the "Submit" option was selected in the "Optimization Process Manager to start the Tosca Structure pre-processor. The “Monitor” was activated to follow the cycles. It should be noted that in the Monitor dialog box, the "Monitor" is enabled to follow the steps of the Abaqus/Standard analysis and the “Kill” option can be used to stop the calculation process.

The "Plot" option can be activated during or at the conclusion of the optimization calculation procedure, see Figure 20. This option enables the visualization of the evolution of both the constraint parameter and the objective function.

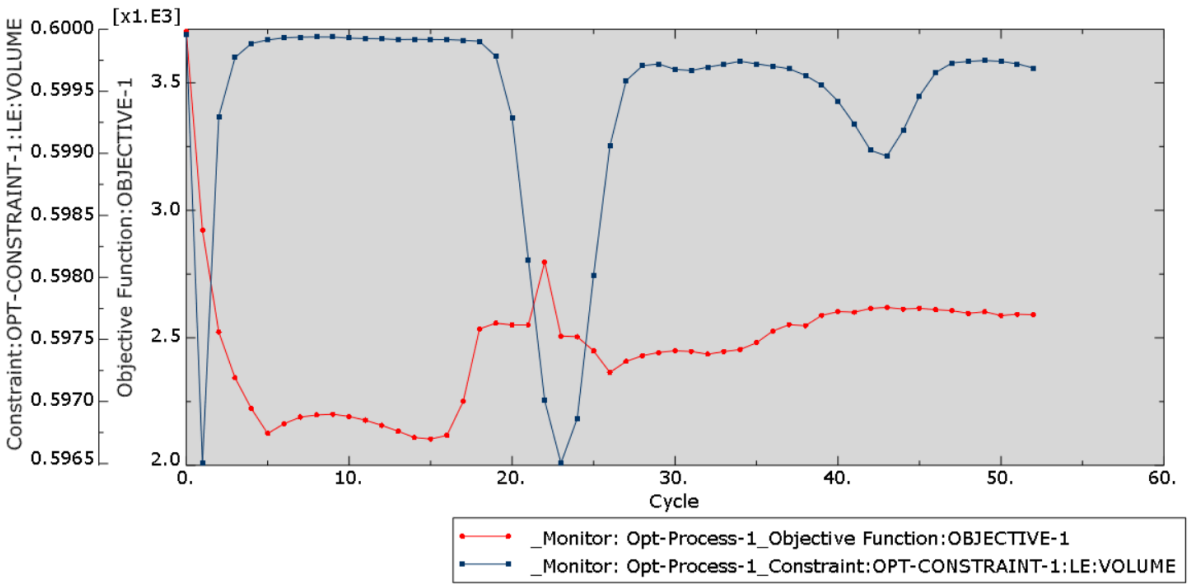

Figure 20. Constraint and the objective function evolution of the optimization.

Upon completion, the "Combine" option must be selected to integrate the optimization results from each cycle. The Submit and Close options must be used consecutively.

In order to draw the "Moment" - "Rotational Displacement" plot, first "Create XY Data" was activated in module "visualization" and "OBD" Field Output" was selected. In the "Variable" folder, "Unique Nodal" is selected for Position, and "UR: Rotational Displacement – UR3" is chosen. Next, on the Elements/Nodes page, "Node Sets" is selected for Method, and "reference_point 2" is selected for Plot. This enables the display of a curve (time, rotational displacement) on the ordinate. Then, the "Create XY Data" option was enabled and "Operate on XY Data" was selected. The "Rotational Displacement" data was already available due to its previous create, only the data for the "Moment" was needed. Therefore, the "Create XY Data" option was selected, and "ODB field output" was chosen. The steps previously presented to generate the UR3 data for the node “reference point 1” were then employed. Two data sets were available for plotting in the "Operate on XY Data" dialogue box: Moment RM3 + Rotational displacement UR3. Ultimately, the "combine " function was selected. Following the selection of the operators and the designation of the dataset’s names, the expression was plotted, see Figure 21. It is necessary to note that for the moment, the values were multiplied by -1 in order to ensure the positivity.

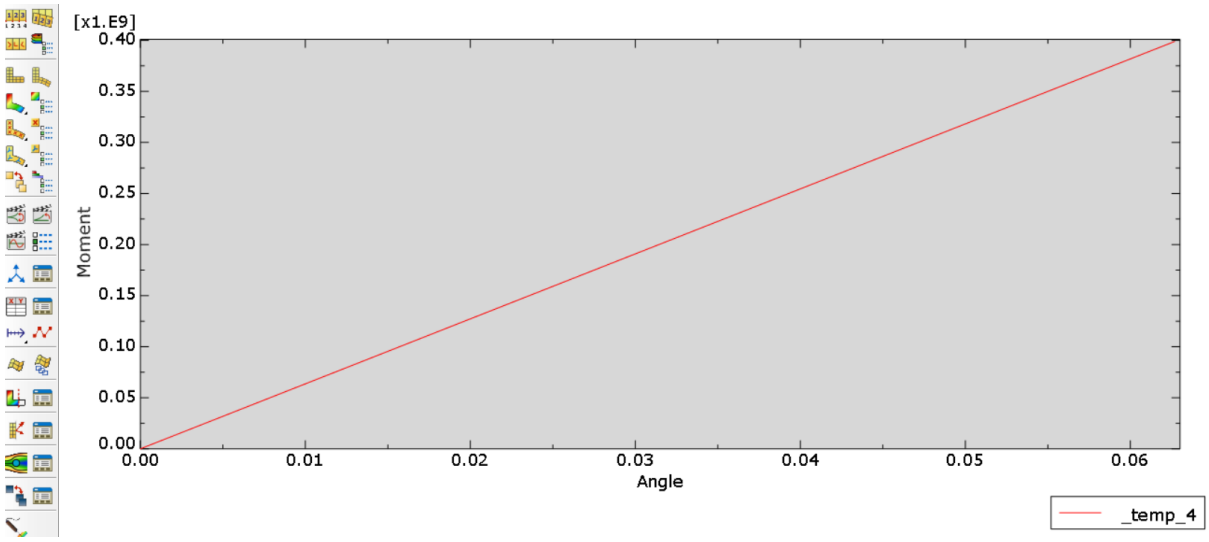

Figure 21. Rotational displacement UR3, Moment RM3 plot

The findings suggest a significant challenge in analyzing large data sets. The selection of optimal points for data extraction has been identified as a pivotal factor in enabling efficient knowledge extraction.

5 Results and Conclusions

5.1 Optimization results with linear analysis

Initially, the optimization process was designed to undergo a minimum of fifty cycles. However, this to be proved insufficient. Therefore, the number of cycles was increased to sixty-five. The total number of cycles required for the optimization process to reach completion was fifty-two. The optimization process was executed on an Intel(R) Core (TM) i5-13420H @ 2.10 GHz processor with 8 GB of RAM. The duration of the optimization process was 33 hours. The results indicate that the primary challenges in optimizing tubular elements subjected to torsion are limited computational resources and temporal constraints.

5.1.1 Reference case: non-optimized pipe

In order to establish reference conditions for the behavior of optimized topologies, the original pipe was analyzed. A finite element mesh of 202,063 S4R elements was defined, refer to Figure 22. The rotational displacements of the linear analysis are displayed in Figure 23, while the stress maps and peak stresses are shown in Figures 24, 25, respectively.

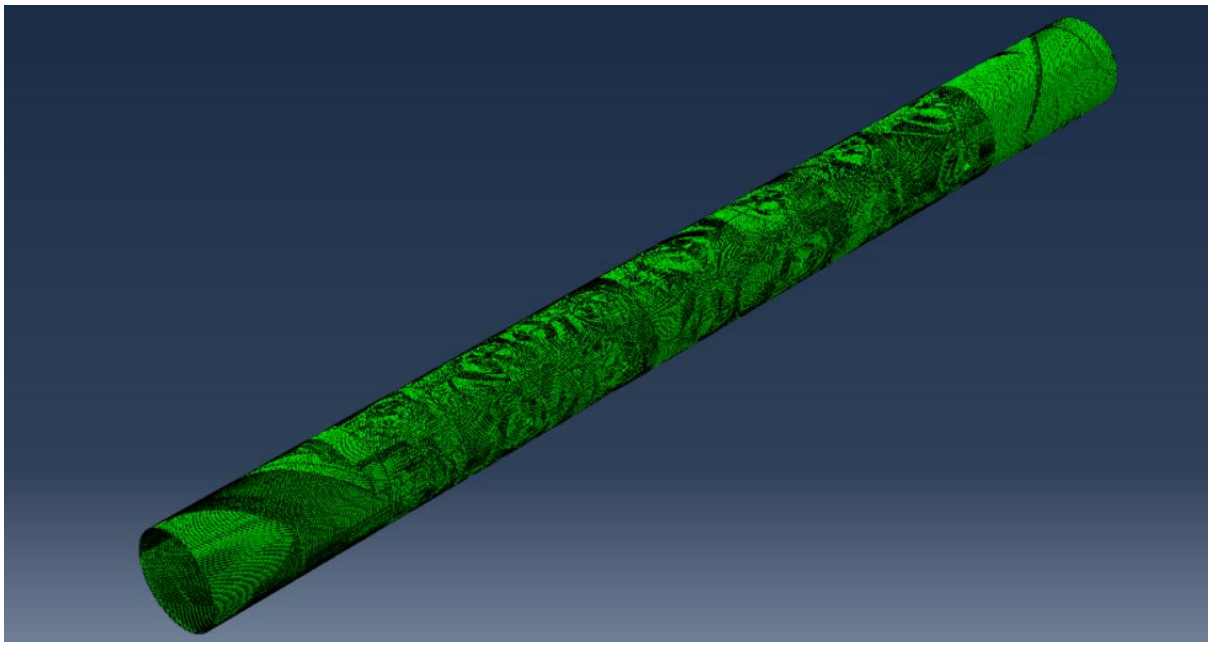

Figure 22. Mesh for the non-optimized pipe

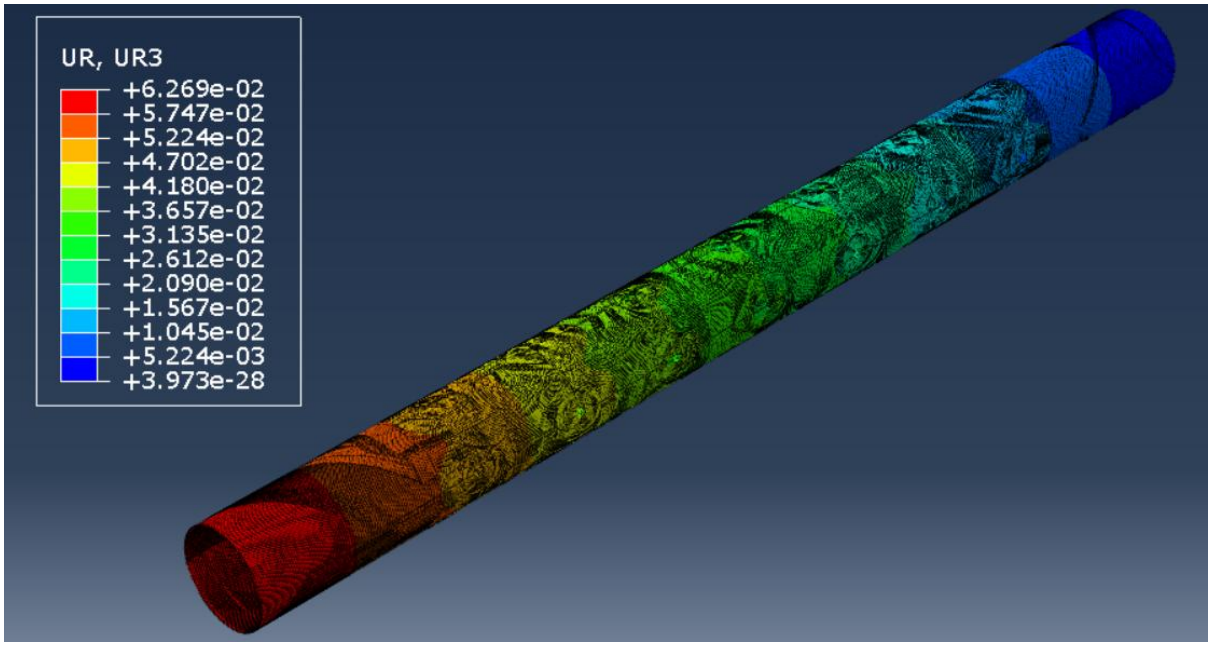

Figure 23. Rotational displacement map for the non-optimized pipe[radian]

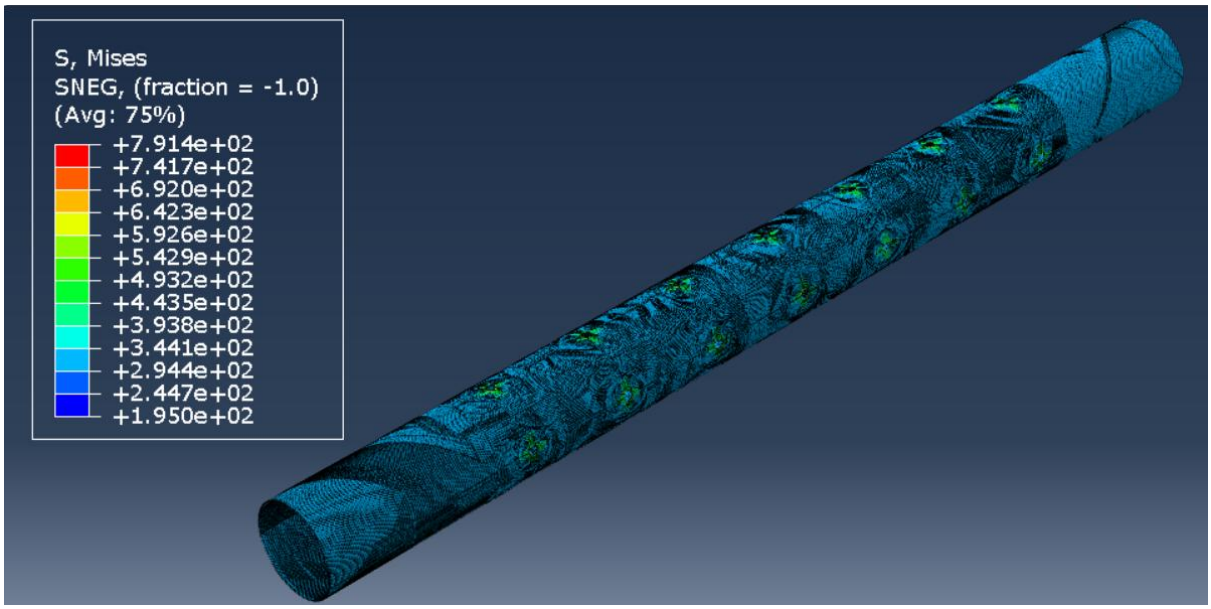

Figure 24. Von Mises stress map [MPa]

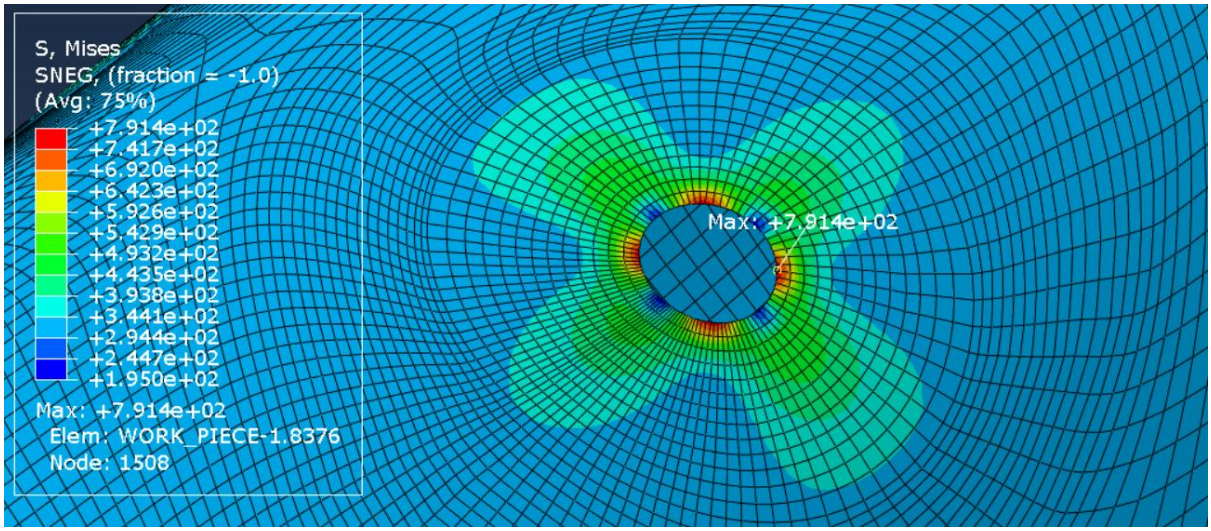

Figure 25. peak values [MPa]

5.1.2 Optimized pipe for the volume fraction (60%).

Once optimized to a fraction of 60% of its original volume (volume reduction 40%) with the goal of minimizing the stress in the region that exhibits maximum stress. The pipe topology is reduced to the depiction in Figure 26. The findings of the study indicate the potential for conducting an optimization procedure that primarily targets zones of lesser engineering usefulness, while exerting minimal impact on the most stressed areas[23],[26]. This observation aligns with the theory that when a torsional load is applied to the pipe induces compressive and tensile stresses in perpendicular helical planes that are 45° from the long axis. It is noteworthy that the tensile stress is maximum in a plane +45° from the long axis and maximum compressive stress occurs at −45°, see Figure 27.

As illustrated in Figure 28, the stress map reveals the distribution of stress throughout the structure. Figure 29 provides a detailed analysis of stress peaks. As Figure 29 indicates, the presence of localized high stresses, which are caused by sudden changes in geometry and sharp corners or edges. These geometric features have the effect of creating stress concentrations.

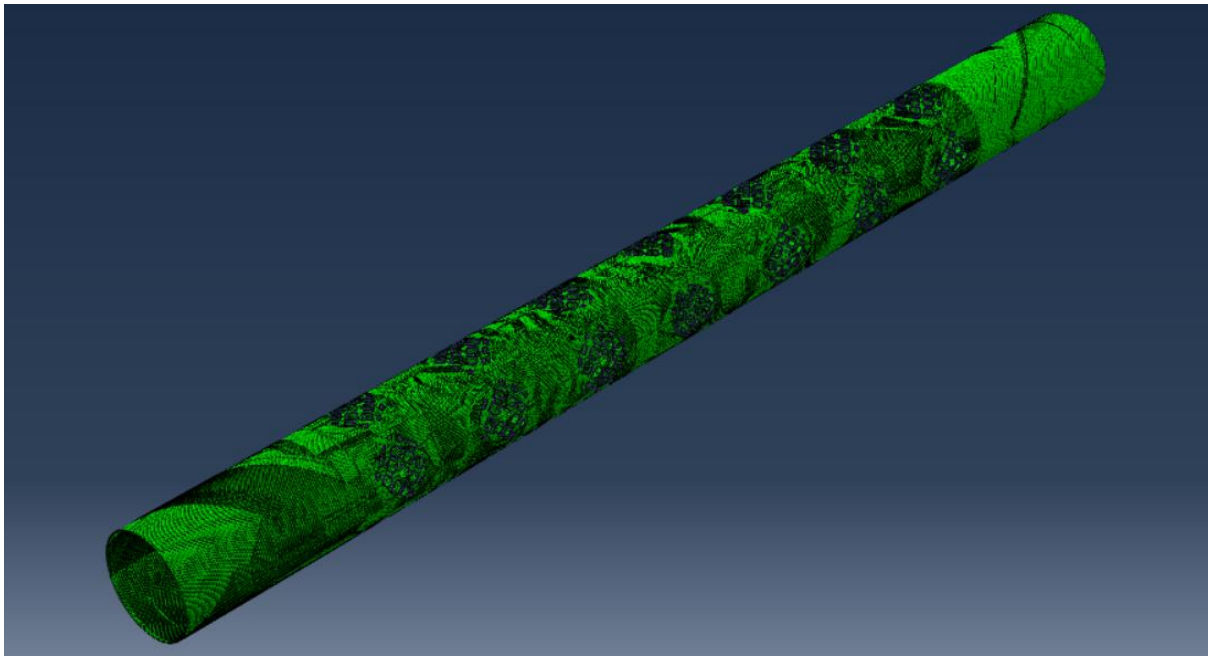

Figure 26. Optimized pipe for the volume fraction of 60%

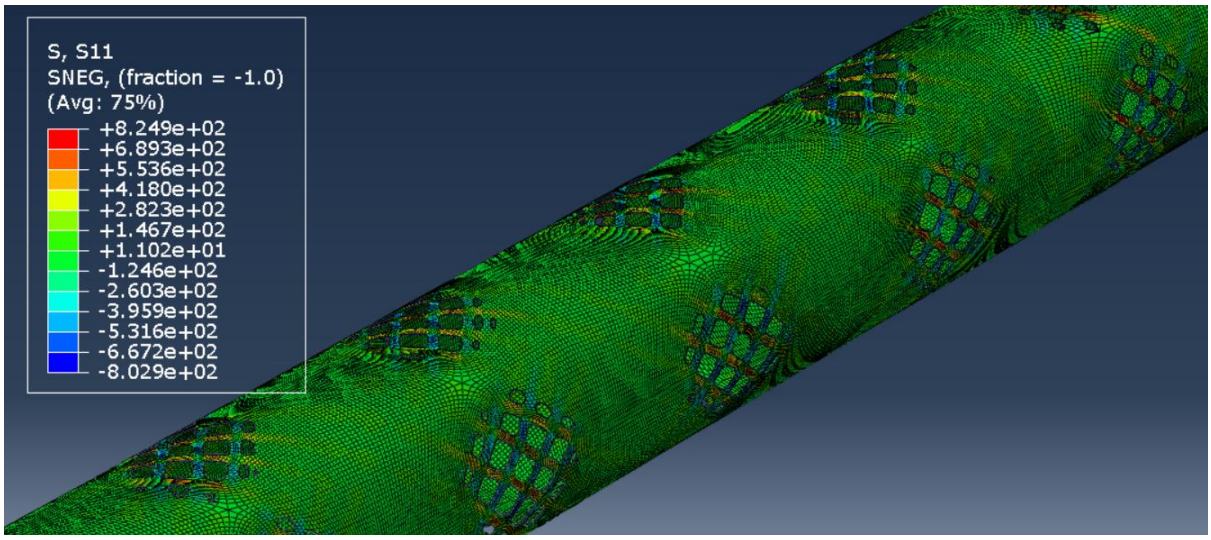

Figure 27 . Stress map S11 [MPa]

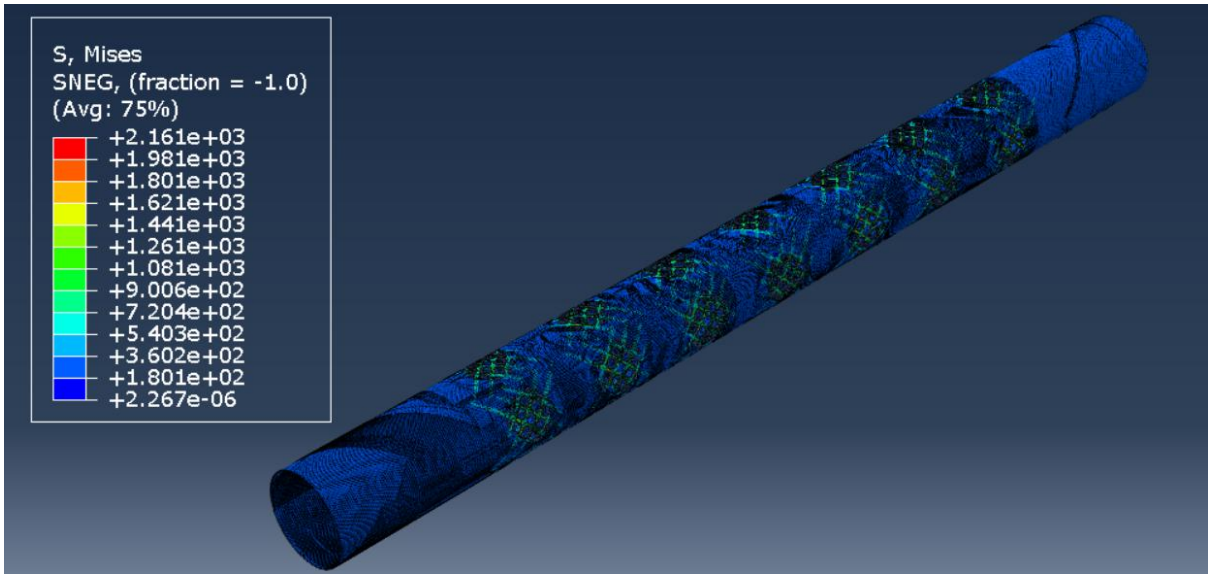

Figure 28. Von Mises stress map [MPa]

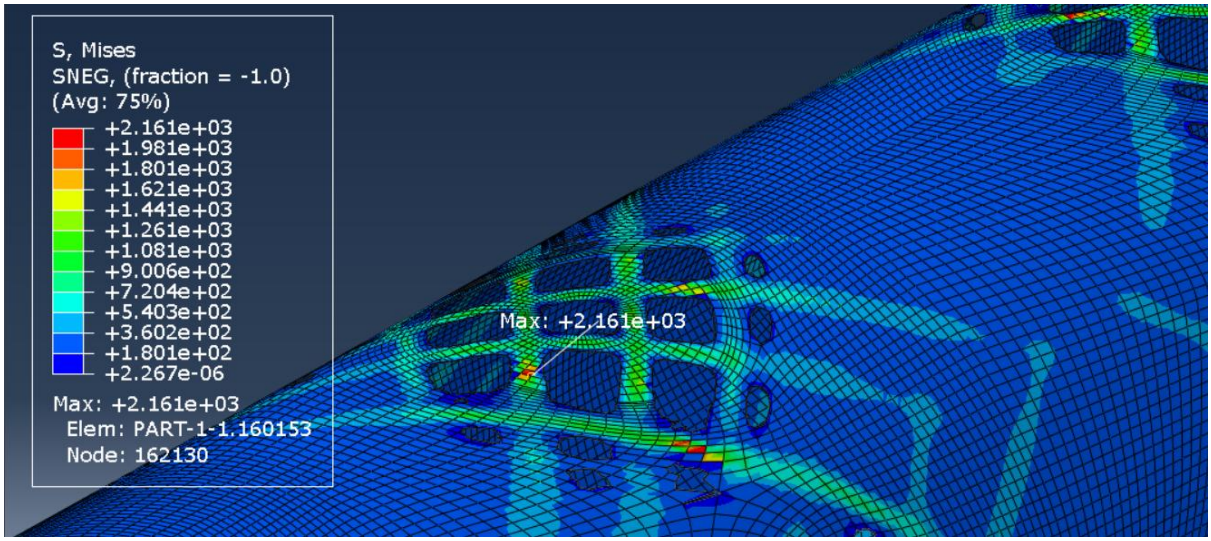

Figure 29. Peak values [MPa]

5.2 non-linear analyses

5.2.1 Reference case: non-optimized pipe

A non-linear analysis of the entire pipe with a 255,000 S4R elements mesh (with 5 mm spacing) was executed on an Intel(R) Core (TM) i5-13420H @ 2.10 GHz processor with 8 GB of RAM. The analysis took two hours and resulted in the rotational displacement and stress maps depicted in Figure 30, 31, and rotational displacement-moment plot shown in Figure 32.

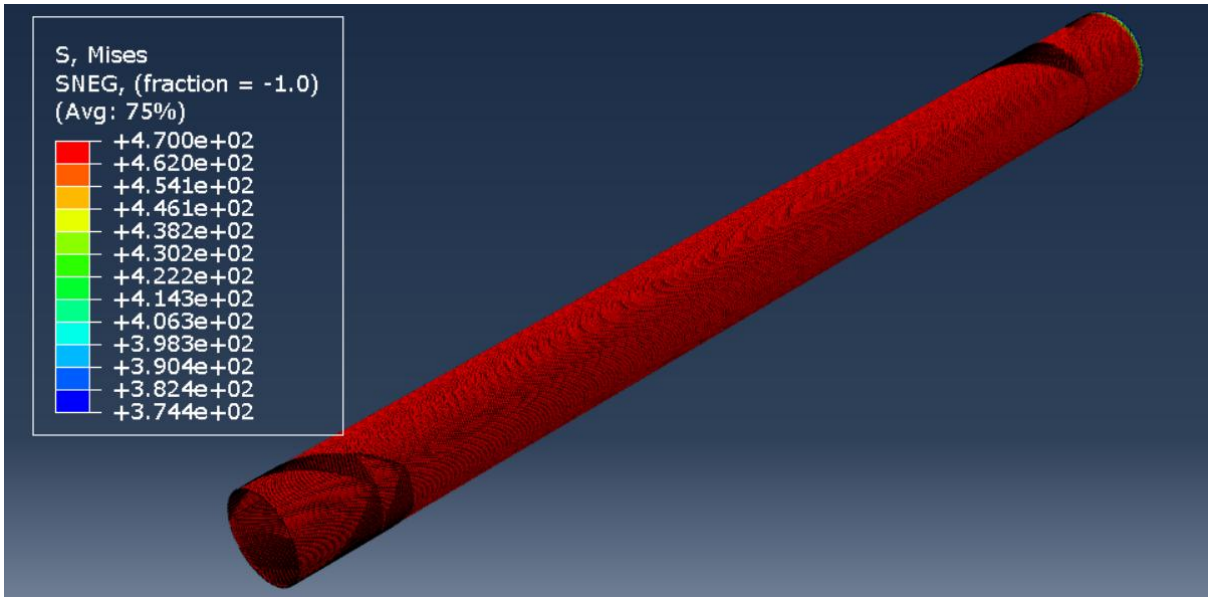

Figure 30. Von Mises stress map [MPa] (entire pipe)

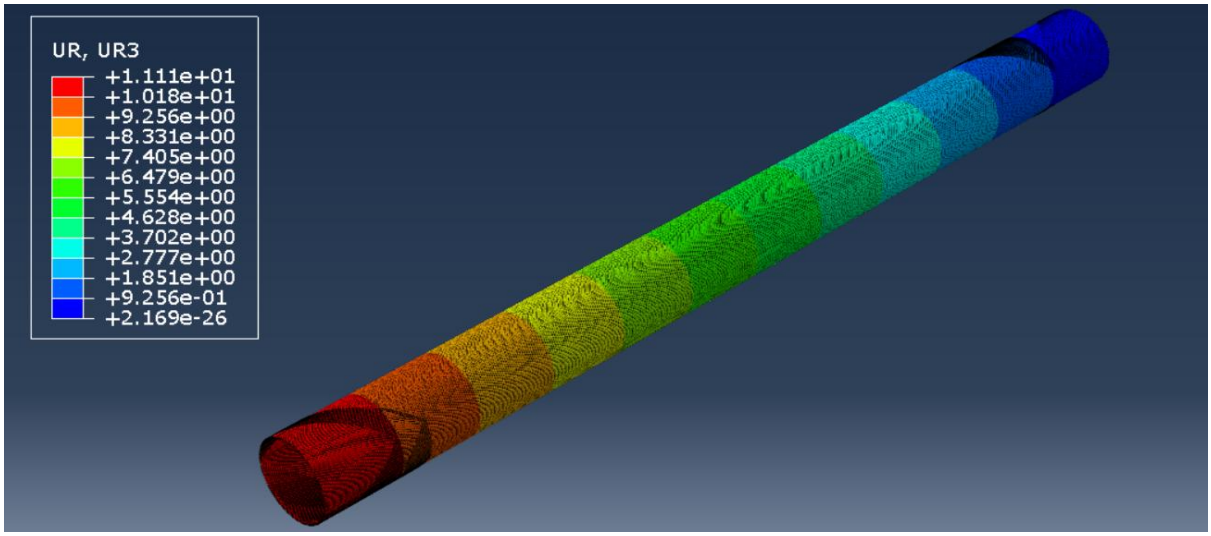

Figure 31. Rotational displacement map [radian] (entire pipe)

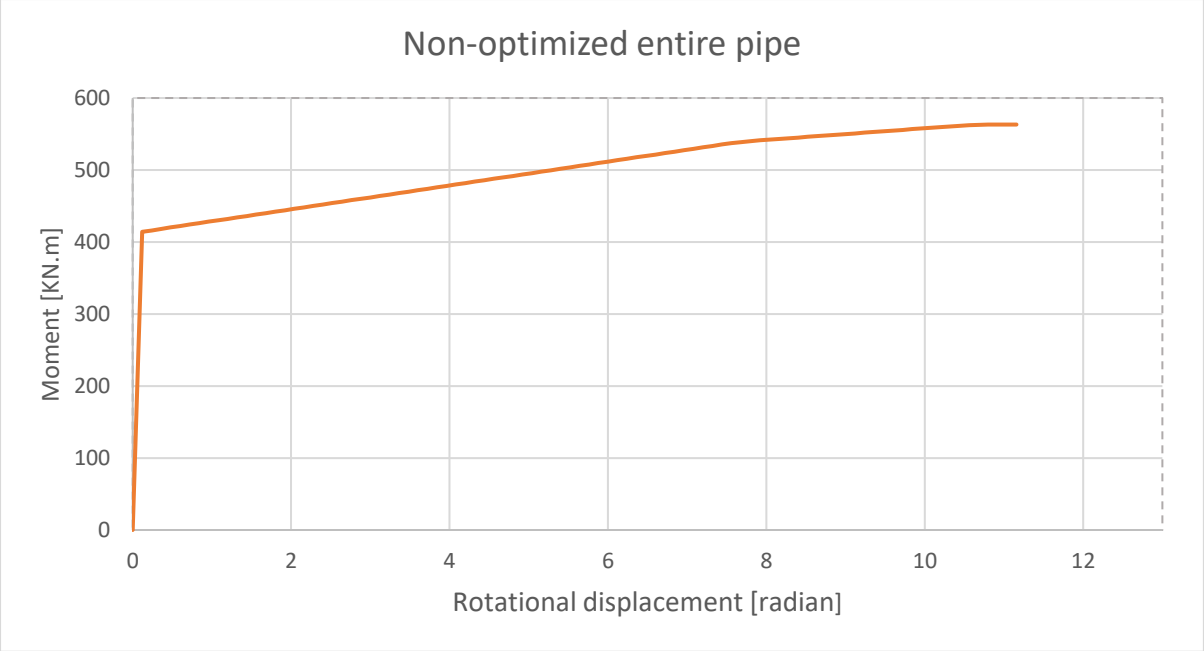

Figure 32. Rotational displacement-moment relation for non-optimized entire pipe

The second model, which incorporated perforations with a diameter of 40 mm with a 207,908 S4R elements mesh (with 5 mm mesh level), was subjected to non-linear analysis and took 9 hours to generate the results depicted in Figure 33,34,35.

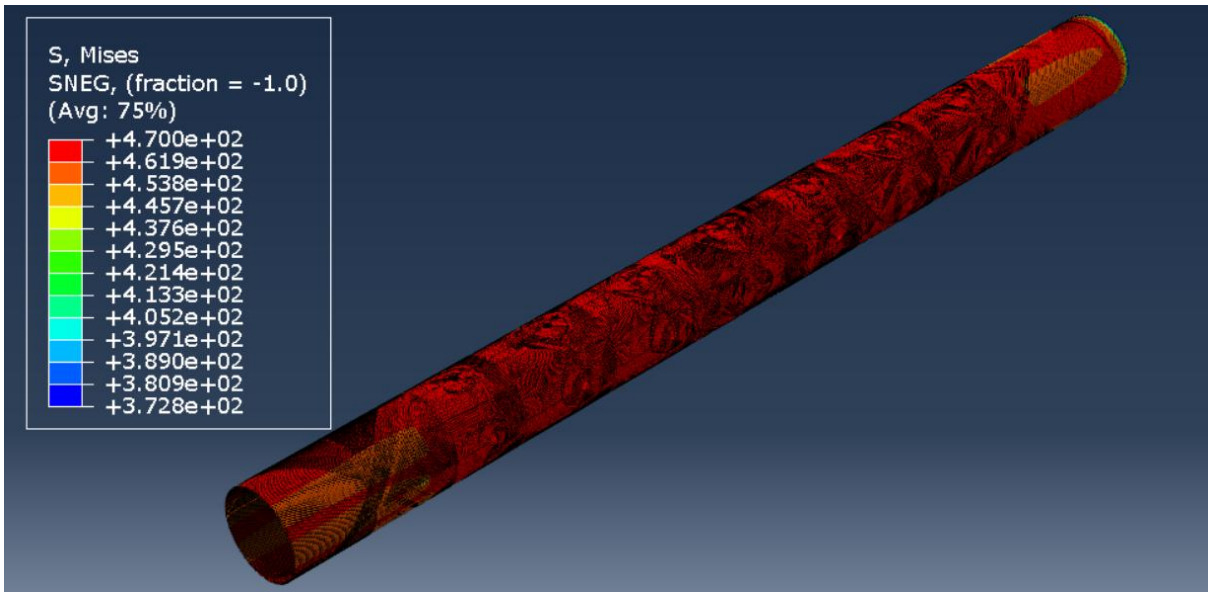

Figure 33. Von Mises stress map [MPa]

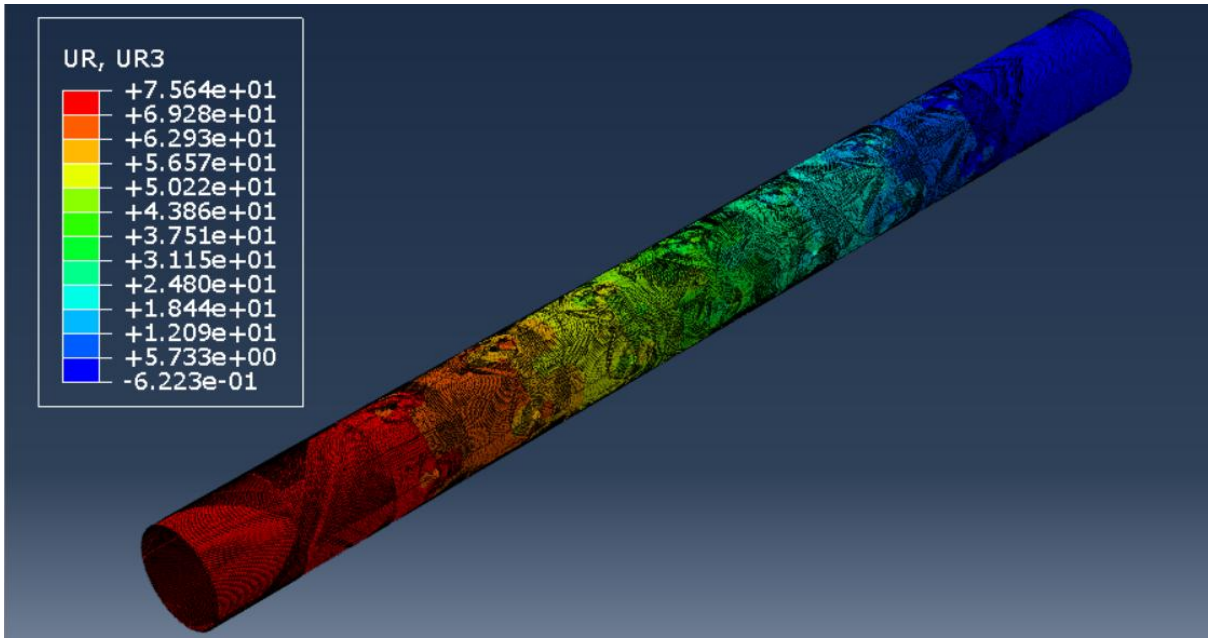

Figure 34. Rotational displacement map [radian]

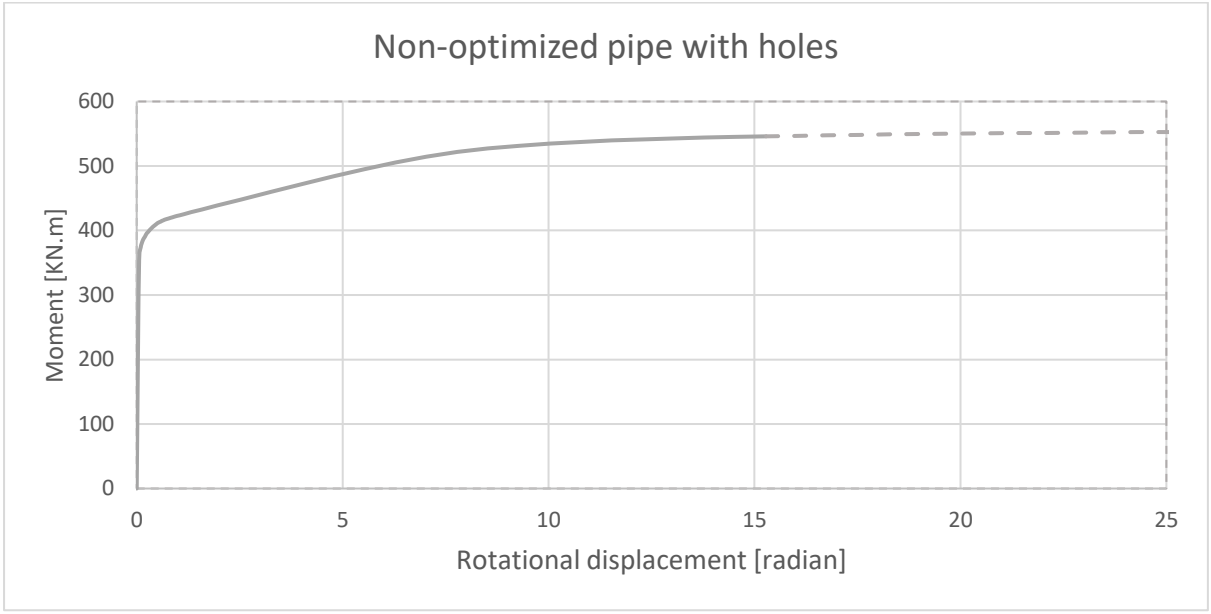

Figure 35.Rotational displacement-moment relation for non-optimized pipe with holes

5.2.2 optimized pipe

A non-linear analysis of the optimized pipe necessitates the extraction of the optimized surface mesh[26],[27]. To do so, one must first access the Job module and select the "Optimization Process Manager. “The "Extract" option in the "Optimization Process Manager" can be utilized to export a surface mesh that has been optimized. The "Extract Surface Mesh" dialogue box will then appear, and the user can enter "Opt_surface" as the output name. "Abaqus input file" has been enabled to generate an Abaqus input file in INP format. The input parameters "iso value " and "filtering" were set to "0.2" and "moderate," respectively. Next, we need to import the optimized geometry into Abaqus from the previously exported file in INP format (Abaqus input file). For this purpose, the Global Standard/Explicit option has been selected. Utilizing the "Import" and "Model" commands within the File menu, the *. Inp file will be selected using the File Filter option to initiate the opening of the file. Then the model is renamed using "save as" from the file menu. The final step entails the application of loading and boundary conditions to the model, followed by a nonlinear analysis, analogous to the previous procedure performed on the non-optimized pipe[28].

A non-linear analysis of the optimized pipe with a 389258 S3R elements mesh was executed on an Intel(R) Core (TM) i5-13420H @ 2.10 GHz processor with 8 GB of RAM. The analysis took fifteen hours and resulted in the rotational displacement , stress maps depicted in Figure 36, 37 , as well as the rotational displacement-moment plot shown in Figure 38.

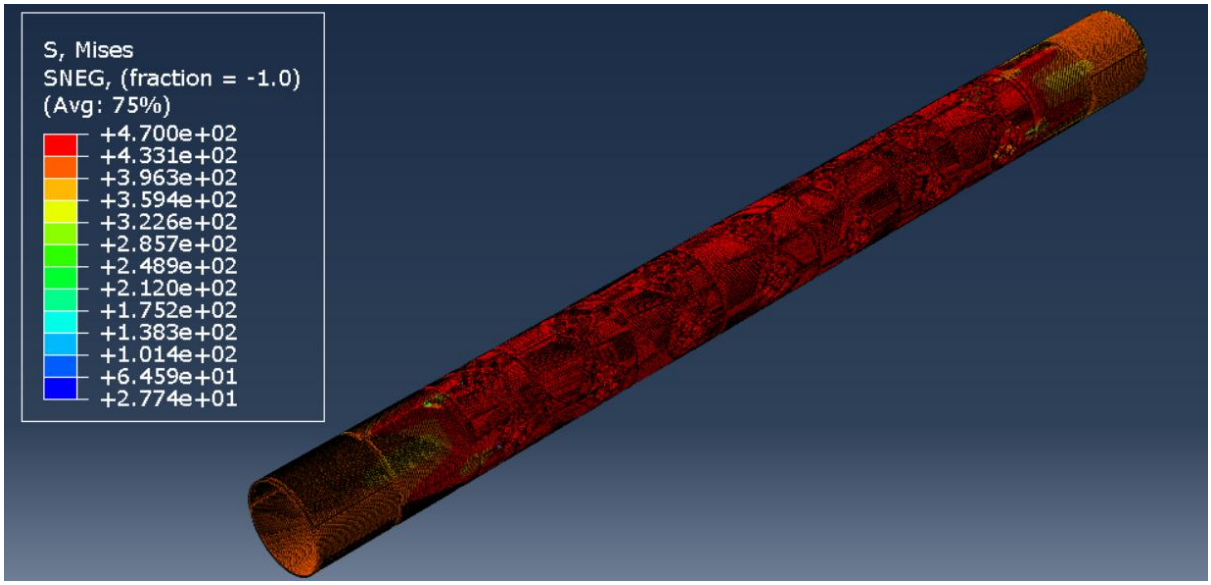

Figure 36. Von Mises stress map [MPa] for optimized pipe

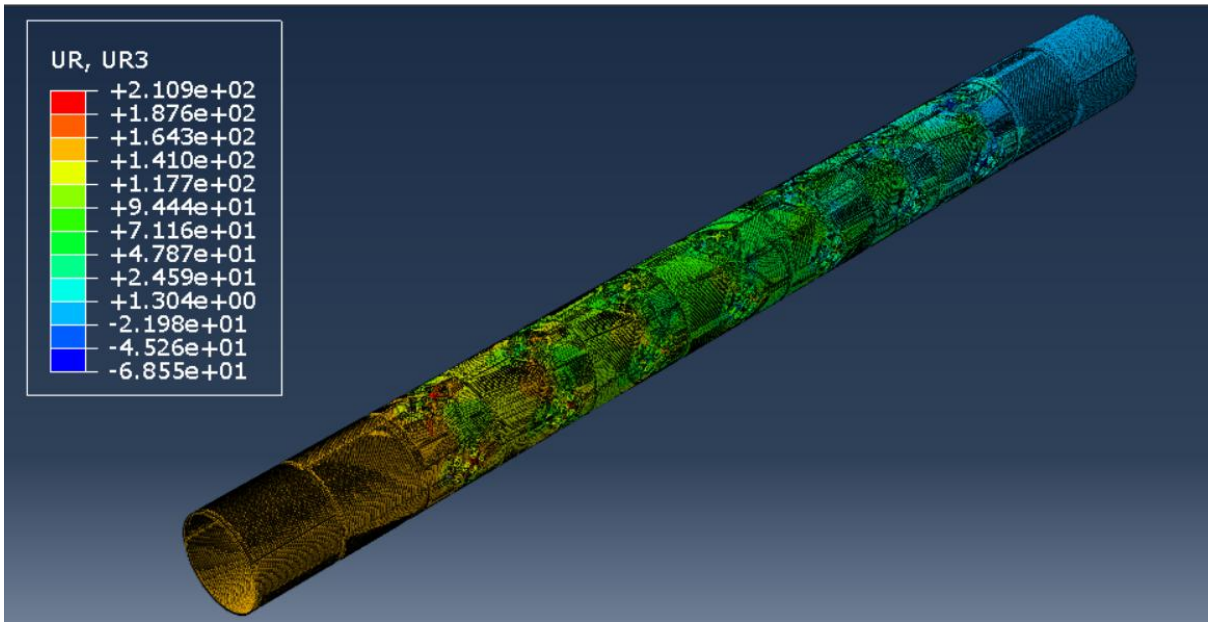

Figure 37. Rotational displacement map [radian] for optimized pipe

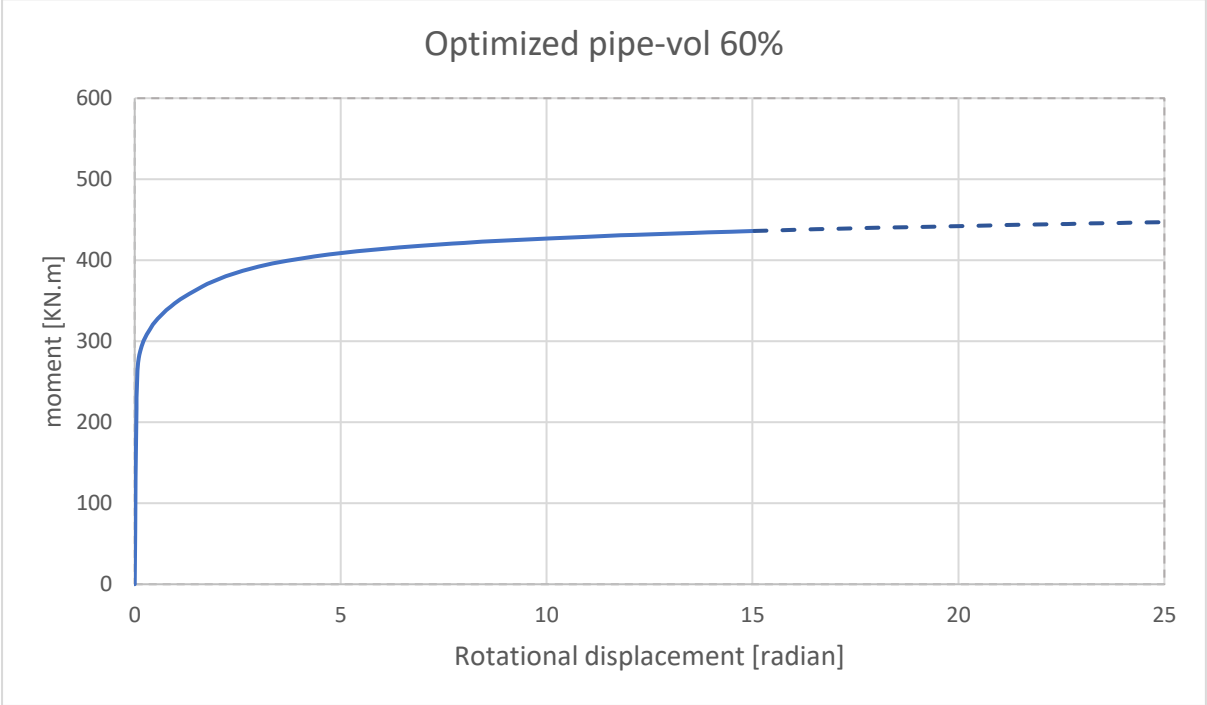

Figure 38. Rotational displacement-moment relation for Optimized pipe-vol 60%

5.3 discussion the results

The findings indicate that decreasing the optimized tube's volume by 40% results in a 32.5% reduction in torque resistance and displays a torque resistance of 280 kN.m. On the other hand, the non-optimized tube with holes, which has undergone a volume reduction, displays a torque resistance of 400 kN.m and a 3.75% reduction in torque resistance.

The evaluation of the displacements associated with the design capacity indicates that the original pipe demonstrates a deformation of 11 radians. However, the optimized pipe did not indicate the deformation because the simulation continued even after the design capacity was reached and did not give a result, as shown in Figure 39 .

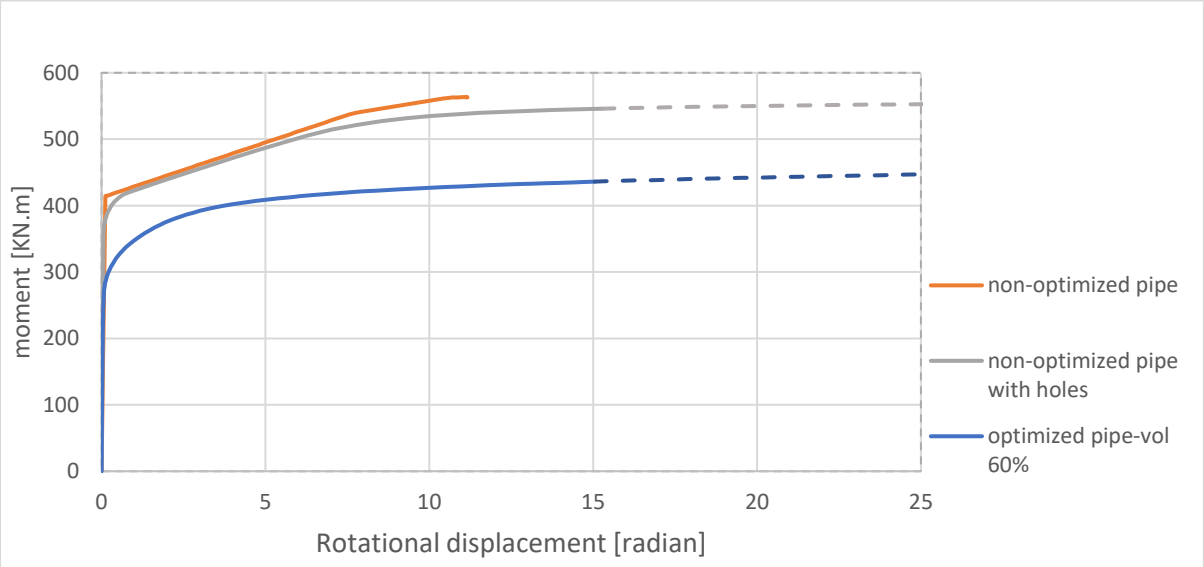

Figure 39. Rotational displacement-moment relation for (non-optimized entire pipe, non-optimized pipe with holes,optimized pipe-vol 60%)

5.4 Conclusions

This dissertation investigates the topological optimization (TO) of tubular elements under torsional loading, focusing on the application of advanced commercial finite element software, typically used in the automotive and aerospace industries, to civil engineering structures. The primary objectives were to evaluate the feasibility of using such software for civil engineering design and to validate the use of nonlinear finite element analysis (NLFEA) following linear elastic optimization A thin-walled commercial pipe was selected as the case study, and the topology was optimized for a volume fraction of 60%. The optimized geometry was then subjected to nonlinear analysis to assess its performance under torsional loading. The results demonstrate that the optimized pipe for a volume fraction of 60% results in a 32.5% reduction in torque resistance.

The findings suggest a substantial challenge in the analysis of extensive data sets. With regard to the latter issue, it has been demonstrated that the selection of the most suitable points from which data should be extracted is paramount to facilitating efficient knowledge extraction.

The findings further underscore that the predominant challenges in optimizing tubular elements under torsional loading are constrained by both computational resources and temporal limitations.

The study highlights the challenges of optimizing tubular elements in civil engineering, particularly under torsional loads, which are more complex to handle compared to tension, compression, or bending.

The study also underlines the necessity for mesh convergence studies to achieve accurate and reliable results, as well as the importance of remeshing and controlling mesh distortions during the optimization process.

Due to the thermal variations of the ocean environment, these elements are subjected to a considerable amount of torsion. It is therefore recommended that the reduction impacts on fatigue life of optimized pipe be evaluated. Accelerated testing under operational conditions is imperative.

The findings indicate that TO has the capacity to attain substantial material savings. This, in turn, results in economic and environmental advantages, including reduced material expenditures, diminished carbon emissions, and curtailed energy consumption during manufacturing and transportation.

6 Bibliography

[1] Huang. Y, Huang. S. Neural network-based prediction of topside mass of an in-service jacket platform. Ocean Engineering.2022: 246: 110554. https://doi.org/10.1016/j.oceaneng.2022.110554

[2] Zhang. Y, Liu. W , Kuang. W , Saneian. M , Bai. Y . Mechanical behaviour analysis of steel strips reinforced thermoplastic pipe under torsion. Ocean Engineering.2024:303: 117655.

a. https://doi.org/10.1016/j.oceaneng.2024.117655

[3] Ibhadode.O, Zhang.Z , Sixt.J , Nsiempba.K .M, Orakwe.J ,Marchese. A. M , Ero., Shahabad.S. I ,Bonakdar. A , Toyserkani E. Topology optimization for metal additive manufacturing: current trends,challenges, and future Outlook Virtual and Physical Prototyping.2023 :18 (1) https://doi.org/10.1080/17452759.2023.2181192

[4] Ballo F. M,Gobbi M ,Mastinu G ,Previati G. Thin-walled tubes under torsion: multi-objective optimal design Optimization and Engineering .2020:21(1): 1-24. 10.1007/S11081-019-09431-8

[5] Alshannaq.A. A. Alshannaq,Tamimi. Abu Qamar. M. F. Sensitivity and Optimization Analysis of Torsional Behavior in Multicellular Thin-Walled Tubes. 2024:10(9) Doi: 10.28991/CEJ-2024-010-09-09

[6] Okumoto.Y , Takeda.Y ,Mano.M ,Okada. T . Finite Element Method. Design of Ship Hull Structures. 2009:125-140. 10.1007/978-3-540-88445-3_7

[7] Sadowski.A. J. On the advantages of hybrid beam-shell structural finite element models for the efficient analysis of metal wind turbine support towers. Finite Elements in Analysis and Design.2019:162: 19-33 .https://doi.org/10.1016/j.finel.2019.05.002

[8] Smith .C.J, Gilbert.M, Todd. I, Derguti.F, Application of layout optimization to the design of additively manufactured metallic components, Struct. Multidiscip. Optim. 2016:54:1297–1313, https://doi.org/10.1007/s00158-016-1426-1.

[9] Ribeiro. T, Bernardo. L, Andrade. J. Topology Optimisation in Structural Steel Design for Additive Manufacturing. Appl. Sci. 2021:11(5):2112.https://doi.org/10.3390/app11052112

[10]Ribeiro. T, Bernardo, R Carrazedo. Finite Element Modelling with Abaqus and Tosca for Topology Optimization of Steel. J Build Des Environ. 2023:1:12362.DOI: 10.37155/2811-0730-0201-3

[11] Pei. L, Hyun. S, Molonaria. J. F, Robbins. M. O.Finite element modeling of elasto-plastic contact between rough surfaces. Journal of the Mechanics and Physics of Solids. 2005: 53(11): 2385-2409. https://doi.org/10.1016/j.jmps.2005.06.008

[12]Rendall .M.A , Hancock. G.J , Rasmussen. K.J.Modal buckling behaviour of long polygonal tubes in uniform torsion using the generalised cFSM . Thin-Walled Structures.2018:128:141-151.https://doi.org/10.1016/j.tws.2017.04.024

[13]Yarlagadda.T , Zhang. Z , Jiang .L , Bhargava. P, Usmani A. Solid isotropic material with thickness penalization – A 2.5D method for structural topology optimization. Computers & Structures.2022:270:106857. https://doi.org/10.1016/j.compstruc.2022.106857

[14] Lee .S, Kim.H, Lieu.Q.X, Lee. J, CNN-based image recognition for topology optimization, Knowl. Base Syst. Knowledge-Based Systems.2020:198: 10588. https://doi.org/10.1016/j.knosys.2020.105887

[15] Ribeiro .T, Bernardo ,R Carrazedo, De Domenico. D . Ultimate capacity and stability of topologically optimised shear plates in compliance with structural Eurocodes. Structures.2023:57:105307.https://doi.org/10.1016/j.istruc.2023.105307

[16] CEN, 2005a. Eurocode 3: Design of steel structures - Part 1-1: General rules and rules for buildings.

[17] Wang.Y , Li.X , Long.K ,Wei.P. Open-Source Codes of Topology Optimization: A Summary for Beginners to Start Their Research. Computer Modeling in Engineering & Sciences.2023 .DOI: 10.32604/cmes.2023.027603

[18] Ribeiro. T, Bernardo. L, Carrazedo .R, De Domenico. D. Eurocode-compliant topology optimisation of steel moment splice connections. J Build Eng 2022;62:105346. https://doi.org/10.1016/j.jobe.2022.105346.

[19] Kaveh .A , Rahami. H, Nonlinear analysis and optimal design of structures via force method and genetic algorithm . Computers & Structures .2006: 84: 770-778. https://doi.org/10.1016/j.compstruc.2006.02.004

[20] Ribeiro .T, Bernardo ,R Carrazedo, De Domenico. D . Topology optimisation of steel connections under compression assisted by physical and geometrical nonlinear fnite element analysis and its application to an industrial case study. Structural and Multidisciplinary Optimization 2024: 67:88 https://doi.org/10.1007/s00158-024-03799-7

[21] Zc.X. Optimal Finite Element Mesh Refinement Based on A-posteriori Error Estimator and the Quality of Mesh.IEEE.2011DOI: 10.1109/ICINIS.2011.33

[22] Raimondo.L, Iannucci.L, Robinson.P, Curtis.P. T. A progressive failure model for mesh-size-independent FE analysis of composite laminates subject to low-velocity impact damage. Composites Science and Technology. 2012:72(5):624–632.DOI: 10.1016/j.compscitech.2012.01.007

[23] Luo.K, Looi.T , Sabetian.Drake.S ,Drake .J. Designing Concentric Tube Manipulators for Stability Using Topology Optimization. IEEE/RJS International Conference on Intelligent Robots and Systems.2018. DOI: 10.1109/IROS.2018.8593806

[24] Yarlagadda.T , Zhang. Z , Jiang .L , Bhargava. P, Usmani A. Solid isotropic material with thickness penalization – A 2.5D method for structural topology optimization. Computers & Structures.2022:270:106857. https://doi.org/10.1016/j.compstruc.2022.106857

[25] Ádány .S , Schafer .B. W .Finite Tube Method for buckling analysis of tubular members using Fourier-approximation for the displacements. Thin-Walled Structures.2025:206: 112672.https://doi.org/10.1016/j.tws.2024.112672.

[26] Bushnell D , Almroth .B.O, Brogan .F . Finite-difference energy method for nonlinear shell analysis. Computers & Structures.1971:1(3):361-387. h://doi.org/10.1016/0045-7949(71)90020-4

[27] Taggart.D.G,Dewhurst.P. Development and validation of a numerical topology optimization scheme for two and three dimensional structures. Advances in Engineering Software.2010:41 (7–8): 910-915 .https://doi.org/10.1016/j.advengsoft.2010.05.004

[28] Wang. H, Zhang .Ch , Qin. Q H, Bai. Y . Tunable compression-torsion coupling effect in novel cylindrical tubular metamaterial architected with boomerang-shaped tetrachiral elements. Materials Today Communications.2022:31:103483.//doi.org/10.1016/j.mtcomm.2022.103483.